

Extra Dimensions at Particle Colliders

Dr. scient. Thesis in Theoretical Particle Physics

by

Erik Wolden Dvergsnes

Thesis submitted in partial fulfillment of requirements for the degree of Dr. scient.



Department of Physics and Technology
University of Bergen
Norway
August 2004

Copyright © 2004 by Erik Wolden Dvergsnes

ISBN 82-497-0227-1

All rights reserved. No part of this publication may be reproduced or transmitted in any form, or by any means, without permission

To Kirsti

Acknowledgments

First and foremost I would like to express my deepest gratitude to my supervisor, Professor Per Osland, for his continuous support, encouragement and excellent advice of both physical and linguistic nature. Thanks for always keeping the door open for numerous questions throughout these years. Our many discussions have been an invaluable contribution to the work presented here.

I have also benefited enormously from the collaboration with Trygve Buanes, Nurcan Öztürk, Alexander A. Pankov and Nello Paver, and I am proud of what we have achieved together.

Thanks to Bjarne Stugu for being a resource when it comes to ATLAS-related questions, as well as helping out with practical and administrative issues, and to Paolo di Vecchia for providing answers to technical details concerning general relativity.

I also have to mention my fellow students at the Physics Department. Thanks to all of you for inspiring discussions during these years.

Finally, my special thanks go to my friends and family in Bergen, Oppdal and Kristiansand, in particular my wife, Kirsti, who adds extra dimensions to my life every day with her presence.

This research has been funded by the Research Council of Norway through the ATLAS project.

Bergen, August 25, 2004

Erik Wolden Dvergsnes

Abstract

This thesis consists of an introduction where we consider different aspects of theories involving extra dimensions, together with four research publications (Papers I–IV) attached at the end. The introductory chapters should serve as background material for better understanding the models on which the articles are based. In Chapt. 4 we also present some plots not included in the papers.

The topic of Papers I–III is *graviton induced bremsstrahlung*. In Paper I we consider the contribution to this process from graviton exchange through gluon-gluon fusion at the LHC, compared to the QED background. Only final-state radiation is considered in Paper I, whereas in Paper II we extend this work to include also the quark-antiquark annihilation with graviton exchange, as well as initial-state radiation for both graviton and Standard Model exchange. Paper III is a study of graviton-induced bremsstrahlung at e^+e^- colliders, including both initial- and final-state radiation.

Paper IV is devoted to a study of the *center-edge asymmetry* at hadron colliders, an asymmetry which previously had been studied for e^+e^- colliders. The center-edge asymmetry can be used as a method of distinguishing between spin-1 and spin-2 exchange, something which will be of major importance if a signal is observed.

Contents

Acknowledgments	v
Abstract	vii
1 Introduction	1
1.1 A Brief History of Gravity and Extra Dimensions	2
1.2 Notation	4
1.3 List of Papers	4
2 Kaluza–Klein Gravitons	7
2.1 From D to 4 Dimensions	7
2.2 Feynman Rules for Kaluza–Klein Gravitons	8
2.2.1 Scalars	10
2.2.2 Vectors	11
2.2.3 Fermions	12
2.2.4 The Graviton Propagator	14
3 Phenomenology of Extra-Dimensional Scenarios	15
3.1 Arkani-Hamed–Dimopoulos–Dvali Scenario	15
3.1.1 Summation over KK Modes	17
3.2 Randall–Sundrum Scenario	20
3.3 Alternative Scenarios	22
3.4 Collider Phenomenology	23
3.5 Experimental Constraints	29
4 Comments on the Papers I–IV	31
4.1 Paper I	31
4.2 Paper II	34
4.3 Paper III	35
4.4 Paper IV	36
5 Summary and Conclusion	39
A Feynman Rules	41

B REDUCE Program Example	43
Bibliography	49
Papers I–IV	

Chapter 1

Introduction

He [The physicist] wants to discuss the gravity law in three dimensions; he never wants the arbitrary force case in n dimensions. So a certain amount of reducing is necessary, because the mathematicians have prepared these things for a wide range of problems. This is very useful, and later on it always turns out that the poor physicist has to come back and say, 'Excuse me, when you wanted to tell me about four dimensions...'

– Richard P. Feynman

Understanding the force of gravity represents a challenge which has puzzled mankind for ages. Naively, one would think that this force, which all of us experience every day is the best known among the forces of nature. Our current understanding of gravity, based on the general theory of relativity, is in excellent agreement with experimental data such as the bending of light around massive objects and the precession of Mercury's perihelia. Furthermore, several predictions, such as frame-dragging and gravitational waves, are about to be tested in the nearest future. But still, we know that there are problems around at the quantum level. Some open questions which still remain are related to:

- Quantum gravity: Although there is no consistent quantum theory of gravitation, and all attempts so far only led to non-renormalizable theories, there are reasons to believe that gravity can be described by exchange of massless spin-2 gravitons. It is however possible to treat quantum gravity as an effective field theory, with a cut-off at the Planck scale.
- Dark energy: Recent observations indicate that the expansion of the Universe is accelerating rather than decelerating. Such behavior cannot be explained by gravity, and therefore a form of energy, called *dark energy*, whose gravity is repulsive is theorized.
- Extra dimensions: Although it seems obvious that we live in a universe with three spatial dimensions and one time dimension, models with extra space dimensions

have gained popularity over the last few years. Such models have the capability of answering yet unanswered questions, and could be realized in nature without being at odds with experimental observations.

In this thesis, some of the theories which address the last of these three questions will be discussed. Many of these theories have the attractive feature that they are testable in existing and upcoming experiments.

Since gravity is always attractive, it is by far the dominant force when it comes to determining the large scale structures of the Universe. However, at the sub-atomic level it is apparently several orders of magnitude weaker than all the other known forces. Therefore it has been common practice to neglect gravity when studying particle physics.

In recent years, several new theories have been proposed as attempts to explain or at least rephrase the so-called *hierarchy problem*¹. By introducing extra spatial dimensions, gravity can be modified to become strong at the electroweak scale. If this is the case, it could be possible to detect effects of gravity at current and future accelerator experiments like the Tevatron, the LHC and also proposed colliders like TESLA and CLIC. In addition, non-accelerator experiments are also capable of contributing to the search for extra dimensions. Needless to say, the discovery of extra dimensions would have far-reaching consequences, since it would change our basic view of the Universe.

Here we shall consider two such theories, and look at how they can manifest themselves in collider experiments by considering specific signatures.

1.1 A Brief History of Gravity and Extra Dimensions

Already in 1687, I. Newton published his famous inverse-square law [1] for the gravitational force between two masses, m_1 and m_2

$$F_g(r) = -G_N \frac{m_1 m_2}{r^2}, \quad (1.1)$$

where G_N is the gravitational constant and r is the distance between the two objects. For centuries, this law experienced a tremendous success in describing gravitational phenomena, from the orbital motion of the moon and the planets to terrestrial objects falling to the ground. There were still deviations which could not be explained by Newton's law of gravity, but it was not clear at the time if these were due to non-gravitational forces or not.

By 1907, H. Minkowski realized that the special relativistic invariance of Maxwell's equations leads to a unification of electric and magnetic forces in a four-dimensional space-time which is a non-euclidean space, known as Minkowski space, in which space and time are not separated, but instead deeply connected. Thus, a connection between unification of forces and the number of dimensions was established.

At a time when the only known forces of nature were gravity and electromagnetism, it probably seemed worthwhile to try unifying these by introducing an extra (spatial)

¹The problem of why the electroweak scale is so different from the Planck scale.

dimension². As early as in 1912, G. Nordström proposed a relativistic theory of gravity, described by a scalar field which coupled to the trace of the energy-momentum tensor [2]. Two years later, in 1914, still before Einstein's general relativity, Nordström unified his theory of gravitation with Maxwell's theory by regarding our four-dimensional space as a surface in a five-dimensional world [3]. Since Nordström's theory failed to describe reality, his ideas did not become very well known.

A. Einstein published his theory of general relativity [4] in 1916, and some years later, in 1919, T. Kaluza, without knowing of Nordström's effort, suggested in a letter to Einstein to solve the five-dimensional field equations of general relativity and obtain Einstein's four-dimensional equations together with Maxwell's equations. His ideas were published two years later [5]. The physical interpretation of this extra dimension was still unclear, until 1926, when O. Klein came up with a possible solution [6]. His proposal was that the fifth dimension may be curled up, or compactified, on a tiny circle, too small to be noticeable.

Since it failed to explain the difference in strength between gravity and electromagnetism, the original Kaluza–Klein idea was forgotten for many years. Moreover, the strong and weak interactions which were discovered later did not fit very well into this picture.

The ultimate dream is still to unify all forces of nature into a *Theory of everything*. For some decades, the best (and only) hope of accomplishing this dream has been superstring or M-theory. Still many aspects of such theories are unknown, but it is clear that they are only consistent in a ten- or eleven-dimensional space-time. Since string theory also encompasses gravity, widely accepted wisdom was to assume a string scale close to the Planck scale, hence the extra dimensions would be extremely compactified, with compactification radii at the Planck length, $\mathcal{O}(10^{-35} \text{ m})$, thus beyond the reach of experiments.

Already in the early eighties, there were speculations that our place in the universe may be constrained to living on a 3-brane³ embedded in a higher-dimensional space [7–9]. In 1990, motivated by perturbative string theory, I. Antoniadis proposed a theory with extra dimensions at the TeV scale [10]. Even phenomenological studies [11] of collider searches for Kaluza-Klein states within the framework of such theories were carried out.

In 1998 however, the situation changed dramatically when N. Arkani-Hamed, S. Dimopoulos and G. R. Dvali proposed a theory of large extra dimensions [12] of the order of 1 mm. Suddenly extra dimensions could be within reach of table-top experiments [13]. A whole new world of different theories opened up, some of which will be described here.

The outline of this thesis is as follows, in Chapt. 2 we derive the Feynman rules of massive Kaluza–Klein gravitons, whereas in Chapt. 3 we discuss some of the theories involving such particles, together with their phenomenology. The four research papers I–IV are discussed in Chapt. 4, and finally, in Chapt. 5 we conclude.

²Extra time-like dimensions would conflict with causality.

³Generally a p -brane is an object with $(p + 1)$ space-time dimensions. String theory contains branes on which particles can be confined or localized.

1.2 Notation

- We assume natural units, $\hbar = c = 1$, such that $\hbar c = 197.3269 \dots \text{ MeV fm} = 1$.
- Gravitational constant: $G_N = 6.71 \dots \times 10^{-39} \text{ GeV}^{-2}$.
- Planck mass: $M_{\text{Pl}} = \frac{1}{\sqrt{G_N}} = 1.22 \dots \times 10^{19} \text{ GeV}$.
- Reduced Planck mass: $\overline{M}_{\text{Pl}} = \frac{M_{\text{Pl}}}{\sqrt{8\pi}}$.
- Graviton coupling: $\kappa = \sqrt{16\pi G_N}$.
- Number of dimensions: $D = 4 + n$, where n is the number of extra dimensions.
- Metric sign convention: $(+, -, -, \dots)$.
- Repeated indices are summed. Latin indices: Upper-case, $M, N \dots$, run over all space-time coordinate labels in D dimensions. Lower-case, $i, j \dots$ label the n extra space dimensions. Greek indices: $\mu, \nu \dots$, are four-dimensional space-time indices.
- Partial derivative: $\partial_\mu \equiv \frac{\partial}{\partial x^\mu}$.
- Equations and figures within the papers I–IV will be referred to by adding the prefix I, II, III or IV, respectively, to their equation and figure number.
- The abbreviation SM will be used for the Standard Model of particle physics.
- The abbreviations ADD, RS and KK will be used for Arkani-Hamed–Dimopoulos–Dvali, Randall–Sundrum and Kaluza–Klein respectively.

1.3 List of Papers

This thesis is based on four scientific publications [14–17] listed below. Paper I is a conference contribution, published in conference proceedings, whereas Papers II–IV are published in refereed journals, and are reprinted here, with permission from the American Physical Society and Springer-Verlag.

Papers I and II are written in collaboration with Per Osland and Nurcan Öztürk, Paper III is written in collaboration with Trygve Buanes and Per Osland, whereas Paper IV is written in collaboration with Per Osland, Alexander A. Pankov and Nello Paver. The papers are attached at the end of this thesis.

- **Paper I:**
E. Dvergsnes, P. Osland and N. Öztürk,
“Characteristics of graviton-induced bremsstrahlung,”
in *Proceedings of 16th International Workshop on High Energy Physics and Quantum Field Theory (QFTHEP 2001)*, edited by M.N. Dubinin and V.I. Savrin, Moscow, Russia, Skobeltsyn Inst. Nucl. Phys., 2001, pp. 54-63, arXiv:hep-ph/0108029.
- **Paper II:**
E. Dvergsnes, P. Osland and N. Öztürk,
“Graviton-induced bremsstrahlung,”
Phys. Rev. D **67**, 074003 (2003) [arXiv:hep-ph/0207221].
©2003 by the American Physical Society.
- **Paper III:**
T. Buanes, E. W. Dvergsnes and P. Osland,
“Graviton-induced bremsstrahlung at e^+e^- colliders,”
Eur. Phys. J. C **35**, 555 (2004) [arXiv:hep-ph/0403267].
© Springer-Verlag / Societa Italiana di Fisica 2004.
- **Paper IV:**
E. W. Dvergsnes, P. Osland, A. A. Pankov and N. Paver,
“Center–edge asymmetry at hadron colliders,”
Phys. Rev. D **69**, 115001 (2004) [arXiv:hep-ph/0401199].
©2004 by the American Physical Society.

Chapter 2

Kaluza–Klein Gravitons

After describing how a D -dimensional massless graviton would appear in four dimensions, we will in this chapter derive the Feynman rules for massive Kaluza–Klein (KK) gravitons. Our discussion will be based on [18] and [19] (for a review, see e.g. [20]). Notation and conventions will be close to those of [19], since this was the notation used in Papers I–III.

The basic assumption in this chapter is that gravity is the only bulk field, meaning it is the only field which propagates in the extra dimensions, whereas all Standard Model (SM) fields are constrained to our four-dimensional world. Here we take the total number of dimensions to be $D = 4 + n$, where n is the number of extra dimensions. Furthermore, the assumption that the n extra dimensions are compactified on a torus, T^n , is made.

This is only one example of how extra dimensions can be introduced, but there are several different ways of doing this, some of which will be presented in the next chapter.

2.1 From D to 4 Dimensions

In general, the graviton field, H_{MN} , is in D dimensions a $D \times D$ symmetric tensor, with $D(D+1)/2$ components. However, for a complete gauge fixing, $2D$ conditions are imposed, thus a D -dimensional massless graviton has $D(D-3)/2$ degrees of freedom. It is obvious that we, from our four-dimensional point of view, must have the same number of degrees of freedom in total. Therefore, a higher-dimensional graviton would result in other particles in addition to the four-dimensional graviton.

Here we discuss the different modes of a higher-dimensional graviton from a four-dimensional point of view. First, the graviton field is decomposed by assuming [19]

$$H_{MN} = V_n^{-\frac{1}{2}} \begin{bmatrix} h_{\mu\nu} + \eta_{\mu\nu}\phi & A_{\mu i} \\ A_{\nu j} & 2\phi_{ij} \end{bmatrix}, \quad (2.1)$$

where $\phi \equiv \phi^i_i$ and $V_n = R^n$ is the volume of the compactified space (with the compactification radius $R/2\pi$). The matrix in Eq. (2.1) is a $D \times D$ matrix with a 4×4 block in the uppermost left corner, $n \times n$ in the lowermost right corner, and $n \times 4$ and $4 \times n$ in its ‘off diagonal’ elements. For an explanation of indices, see Sect. 1.2.

Requiring all fields to be periodic in the extra-dimensional coordinates allows for a Fourier expansion

$$h_{\mu\nu}(x, y) = \sum_{\vec{n}} h_{\mu\nu}^{\vec{n}}(x) e^{2\pi i \vec{n} \cdot \vec{y}/R}, \quad (2.2)$$

with similar expansions for ϕ_{ij} and $A_{\mu i}$, where x represents the four-dimensional coordinates, whereas \vec{y} represents those of the extra dimensions. Furthermore, \vec{n} is the excitation level.

From a higher-dimensional Lagrangian with the equation of motion for a massless graviton in D dimensions, a KK reduction is performed using the Fourier expansion in Eq. (2.2), and four-dimensional equations of motion for the KK modes are obtained [19]. We shall not go into detail here, but instead quote the result. After a redefinition of the fields into physical fields, $\tilde{h}_{\mu\nu}^{\vec{n}}$, $\tilde{A}_{\mu i}^{\vec{n}}$ and $\tilde{\phi}_{ij}^{\vec{n}}$, it can be shown that at each KK level, the different fields represent a massive spin-2 particle, $n - 1$ massive spin-1 particles and $n(n - 1)/2$ massive spin-0 particles. For the zero mode we have the massless graviton, n massless spin-1 particles, and $n(n + 1)/2$ massless spin-0 particles. Note that summation of the degrees of freedom at each KK level gives the same number as for the massless D -dimensional graviton.

The mass of these KK particles at a given excitation level, \vec{n} , is given by

$$m_{\vec{n}}^2 = \frac{4\pi^2 \vec{n}^2}{R^2}, \quad (2.3)$$

thus they form a so-called KK tower with equidistant mass separation.

2.2 Feynman Rules for Kaluza–Klein Gravitons

In this section, Feynman rules for KK gravitons are derived. Since these rules will be identical for every graviton in the KK tower, except from the different masses, we shall for simplicity restrict ourselves to consider exchange of a single massive graviton with couplings to fermions and bosons of the SM. The masses of the SM particles are kept here, but will be neglected later.

Let the induced 4-dimensional metric tensor be

$$\begin{aligned} g_{\mu\nu} &\equiv \eta_{\mu\nu} + \kappa(h_{\mu\nu} + \eta_{\mu\nu}\phi), \\ g^{\mu\nu} &= \eta^{\mu\nu} - \kappa(h^{\mu\nu} + \eta^{\mu\nu}\phi) + \mathcal{O}(\kappa^2), \end{aligned} \quad (2.4)$$

where $\eta_{\mu\nu}$ is the metric of Minkowski space, $h_{\mu\nu}$ represents the gravitational field, ϕ is a scalar field (dilaton) and $\kappa = \sqrt{16\pi G_N}$. The determinant of the metric tensor can to first order in κ be expressed as

$$\begin{aligned} g &\equiv |g_{\mu\nu}| = e^{\log |\eta_{\mu\nu} + \kappa(h_{\mu\nu} + \eta_{\mu\nu}\phi)|} = e^{\log |\eta_{\mu\nu}|} e^{\log |\eta^{\rho}_{\nu} + \kappa(h^{\rho}_{\nu} + \eta^{\rho}_{\nu}\phi)|} \\ &= -e^{\text{Tr} \log [\eta^{\rho}_{\nu} + \kappa(h^{\rho}_{\nu} + \eta^{\rho}_{\nu}\phi)]} = -e^{\text{Tr} [\kappa(h^{\rho}_{\nu} + \eta^{\rho}_{\nu}\phi) + \mathcal{O}(\kappa^2)]} = -e^{\kappa(h + 4\phi) + \mathcal{O}(\kappa^2)} \\ &= -1 - \kappa(h + 4\phi) + \mathcal{O}(\kappa^2), \end{aligned} \quad (2.5)$$

where $h = h^\mu{}_\mu$, thus

$$\sqrt{-g} = 1 + \frac{\kappa}{2}h + 2\kappa\phi + \mathcal{O}(\kappa^2). \quad (2.6)$$

The starting point for deriving the Feynman rules for KK gravitons is the minimal gravitational coupling of scalars, vectors and fermions, described by the action

$$\mathcal{S} = \int d^4x \sqrt{-g} \mathcal{L}(g, S, V, F), \quad (2.7)$$

where $\mathcal{L}(g, S, V, F)$ is the Lagrangian density of the SM. The reason for introducing the factor $\sqrt{-g}$ in the action is that together with d^4x it forms an invariant volume element under general coordinate transformations.

After using Eq. (2.6) we obtain the $\mathcal{O}(\kappa)$ term

$$\mathcal{S}_\kappa = -\frac{\kappa}{2} \int d^4x (h^{\mu\nu} T_{\mu\nu} + \phi T^\mu{}_\mu), \quad (2.8)$$

where the energy-momentum tensor, $T_{\mu\nu}$, is defined as

$$T_{\mu\nu} \equiv \frac{2}{\sqrt{-g}} \frac{\delta(\sqrt{-g}\mathcal{L})}{\delta g^{\mu\nu}} = \left(-\eta_{\mu\nu}\mathcal{L} + 2\frac{\delta\mathcal{L}}{\delta g^{\mu\nu}} \right) \Big|_{g=\eta}. \quad (2.9)$$

The last term represents variation of the Lagrangian with respect to the metric tensor, $g^{\mu\nu}$, and the restriction $g = \eta$ is made not to include terms of higher order than $\mathcal{O}(\kappa)$. After substituting for the physical fields according to the redefinition of fields mentioned in the previous section, one gets [19]

$$\mathcal{S}_\kappa = -\frac{\kappa}{2} \sum_{\vec{n}} \int d^4x (\tilde{h}^{\mu\nu, \vec{n}} T_{\mu\nu} + \omega \tilde{\phi}^{\vec{n}} T^\mu{}_\mu), \quad (2.10)$$

where $\omega = \sqrt{\frac{2}{3(n+2)}}$. Note that the vector KK modes, $A_{\mu i}$, have now decoupled, and the scalar (dilaton), ϕ , only couples through the trace of the energy momentum tensor.

When deriving Feynman rules we shall in the following use the notation $h^{\mu\nu}$ instead of $\tilde{h}^{\mu\nu, \vec{n}}$. Furthermore, we work in the gauge where terms involving the gauge-fixing parameter, ξ , vanish¹. In the limit of massless particles, the trace of the energy momentum tensor vanishes at tree-level, thus the scalar KK modes, which couple only through the trace of the energy momentum tensor, also decouple in this limit. For simplicity we therefore also neglect terms involving the scalar KK modes, $\tilde{\phi}^{\vec{n}}$. Thus, the rest of this chapter is devoted to deriving the Feynman rules arising from the action

$$\mathcal{S}_\kappa^{\vec{n}} = -\frac{\kappa}{2} \int d^4x h^{\mu\nu} T_{\mu\nu}, \quad (2.11)$$

where $h^{\mu\nu}$ is a massive \vec{n} -level KK graviton.

¹A gauge-fixing term involving ξ is introduced in the (vector) Lagrangian density in [19].

2.2.1 Scalars

The Lagrangian density for a complex scalar field can be written

$$\mathcal{L}_S = \frac{1}{2}g^{\mu\nu}[(D_\mu\Phi)^\dagger(D_\nu\Phi) + (D_\nu\Phi)^\dagger(D_\mu\Phi)] - m_\Phi^2\Phi^\dagger\Phi, \quad (2.12)$$

where we have symmetrized the first term in $\mu \leftrightarrow \nu$. The gauge covariant derivative is defined as

$$\begin{aligned} D_\mu &= \partial_\mu + ieQA_\mu, & \text{abelian case,} \\ D_\mu &= \partial_\mu + igT^a A_\mu^a, & \text{non-abelian case,} \end{aligned} \quad (2.13)$$

where g is the gauge coupling and T^a are the group generators. In the abelian case, Q is the charge of the scalar measured in units of the positron charge, e . Given the above Lagrangian we obtain the energy-momentum tensor for a scalar,

$$T_{\mu\nu}^S = -\eta_{\mu\nu}[(D^\rho\Phi)^\dagger(D_\rho\Phi) - m_\Phi^2\Phi^\dagger\Phi] + (D_\mu\Phi)^\dagger(D_\nu\Phi) + (D_\nu\Phi)^\dagger(D_\mu\Phi). \quad (2.14)$$

From Eqs. (2.10) and (2.14), we find the following interaction Lagrangian density which describes the couplings between scalars and a massive KK graviton

$$\mathcal{L}_S^{\text{int}} = -\frac{\kappa}{2} \left\{ (h^{\mu\nu} - \frac{1}{2}\eta^{\mu\nu}h)[(D_\mu\Phi)^\dagger(D_\nu\Phi) + (D_\nu\Phi)^\dagger(D_\mu\Phi)] + hm_\Phi^2\Phi^\dagger\Phi \right\}, \quad (2.15)$$

where Φ is a complex scalar field and $h^{\mu\nu}$ is a massive spin-2 KK field.

Using this interaction Lagrangian density, we can read off the corresponding Feynman vertex in the following way: First, the combination of fields in each term tells us which vertex it contributes to, e.g. $h^{\mu\nu}\Phi^\dagger\Phi$ -terms give us the graviton-scalar-scalar vertex. We also have to include a factor i when going from the interaction Lagrangian to the vertex, and furthermore we use the relation $\partial_\mu\Phi = -ik_\mu\Phi$, where k_μ is the 4-momentum coming into the vertex.

From Eq. (2.15) we get the following Feynman vertex for the graviton-scalar-scalar coupling:

$$\begin{aligned} h^{\mu\nu}\Phi^\dagger\Phi : & \quad -i\frac{\kappa}{2}h^{\mu\nu}[(\partial_\mu\Phi)^\dagger(\partial_\nu\Phi) + (\partial_\nu\Phi)^\dagger(\partial_\mu\Phi) - \eta_{\mu\nu}\eta_{\rho\sigma}(\partial^\rho\Phi)^\dagger(\partial^\sigma\Phi) + \eta_{\mu\nu}m_\Phi^2\Phi^\dagger\Phi] \\ & \Rightarrow -i\frac{\kappa}{2}[\eta_{\mu\sigma}\eta_{\nu\rho}(ik_2^\sigma)(-ik_1^\rho) + \eta_{\mu\rho}\eta_{\nu\sigma}(ik_2^\sigma)(-ik_1^\rho) \\ & \quad - \eta_{\mu\nu}\eta_{\rho\sigma}(ik_2^\sigma)(-ik_1^\rho) + \eta_{\mu\nu}m_\Phi^2] \\ & = -i\frac{\kappa}{2}(m_\Phi^2\eta_{\mu\nu} + C_{\mu\nu\rho\sigma}k_1^\rho k_2^\sigma), \end{aligned} \quad (2.16)$$

with $C_{\mu\nu\rho\sigma}$ as defined in Appendix A, and the momenta in the direction indicated by the arrows in Fig. A.2. We have omitted the Kronecker delta, δ_{mn} , given in [19]. The graviton-scalar-scalar-vector coupling is also contained in the interaction Lagrangian, but since we will not use the Feynman rules for scalars, it is not derived here.

2.2.2 Vectors

The Lagrangian density for a hermitian massive abelian gauge (vector) field can be written

$$\mathcal{L}_V = -\frac{1}{4}g^{\mu\rho}g^{\nu\sigma}F_{\mu\nu}F_{\rho\sigma} + \frac{1}{2}m_A^2g^{\mu\nu}A_\mu A_\nu. \quad (2.17)$$

Here we shall only derive the Feynman rules for the abelian case, but the non-abelian case is analogous, provided we substitute $F_{\mu\nu}$ and A_μ with $F_{\mu\nu}^a$ and A_μ^a , where the field-strength tensors have the following definition

$$\begin{aligned} F_{\mu\nu} &= \partial_\nu A_\mu - \partial_\mu A_\nu, & \text{abelian case,} \\ F_{\mu\nu}^a &= \partial_\nu A_\mu^a - \partial_\mu A_\nu^a + gf^{abc}A_\mu^b A_\nu^c, & \text{non-abelian case,} \end{aligned} \quad (2.18)$$

and f^{abc} are the structure constants of the gauge group. In addition, the non-abelian case has the possibility of having 4-point and 5-point vertices.

To find the energy momentum tensor in the vector case, we need to find the variation of the Lagrangian with respect to the metric, $g^{\mu\nu}$,

$$\begin{aligned} \delta\mathcal{L}_V &= -\frac{1}{4}(\delta g^{\mu\rho}g^{\nu\sigma} + g^{\mu\rho}\delta g^{\nu\sigma})F_{\mu\nu}F_{\rho\sigma} + \frac{1}{2}m_A^2\delta g^{\mu\nu}A_\mu A_\nu \\ &= -\frac{1}{4}[(g^{\rho\sigma}F_{\mu\rho}F_{\nu\sigma} + g^{\sigma\rho}F_{\sigma\nu}F_{\rho\mu}) - 2m_A^2A_\mu A_\nu]\delta g^{\mu\nu} \\ &= -\frac{1}{4}[(F_\mu{}^\sigma F_{\nu\sigma} + F_{\sigma\nu}F_\mu{}^\sigma) - 2m_A^2A_\mu A_\nu]\delta g^{\mu\nu} \\ &= -\frac{1}{2}[F_\mu{}^\rho F_{\nu\rho} - m_A^2A_\mu A_\nu]\delta g^{\mu\nu}, \end{aligned} \quad (2.19)$$

where we have used the fact that $F_{\mu\nu}$ is antisymmetric in $\mu \leftrightarrow \nu$, and also renamed and interchanged some indices.

The energy-momentum tensor for the vector field in Eq. (2.17) now becomes

$$T_{\mu\nu} = \eta_{\mu\nu} \left(\frac{1}{4}F^{\rho\sigma}F_{\rho\sigma} - \frac{1}{2}m_A^2A^\rho A_\rho \right) - F_\mu{}^\rho F_{\nu\rho} + m_A^2A_\mu A_\nu, \quad (2.20)$$

and from Eq. (2.10) we get the interaction Lagrangian density for KK gravitons

$$\mathcal{L}_V^{\text{int}} = -\frac{\kappa}{2} \left[\left(\frac{1}{4}h\eta^{\mu\nu} - h^{\mu\nu} \right) F_\mu{}^\rho F_{\nu\rho} - \frac{1}{2}(h\eta^{\mu\nu} - 2h^{\mu\nu})m_A^2A_\mu A_\nu \right]. \quad (2.21)$$

This results in the following graviton-vector-vector Feynman vertex

$$\begin{aligned} h^{\mu\nu}A^\rho(k_1)A^\sigma(k_2) : & \quad -i\frac{\kappa}{2}h^{\mu\nu} \left[\left(\frac{1}{4}\eta_{\mu\nu}\eta_{\rho\sigma} - \eta_{\mu\rho}\eta_{\nu\sigma} \right) (\partial^\lambda A^\rho - \partial^\rho A^\lambda)(\partial_\lambda A^\sigma - \partial^\sigma A_\lambda) \right. \\ & \quad \left. - \frac{1}{2}m_A^2(\eta_{\mu\nu}\eta_{\rho\sigma} - 2\eta_{\mu\rho}\eta_{\nu\sigma})A^\rho A^\sigma \right] \\ \Rightarrow & \quad -i\frac{\kappa}{2} \left[\frac{1}{2}(-\eta_{\mu\nu}\eta_{\rho\sigma}(k_1 \cdot k_2) + \eta_{\mu\nu}k_{1\sigma}k_{2\rho} + \eta_{\mu\nu}k_{2\rho}k_{1\sigma} - \eta_{\mu\nu}\eta_{\rho\sigma}(k_1 \cdot k_2)) \right. \\ & \quad \left. + 2(\eta_{\mu\rho}\eta_{\nu\sigma}(k_1 \cdot k_2) - \eta_{\mu\rho}k_{1\sigma}k_{2\nu} - \eta_{\nu\sigma}k_{1\mu}k_{2\rho} + k_{1\mu}k_{2\nu}\eta_{\rho\sigma}) \right. \\ & \quad \left. - m_A^2(\eta_{\mu\nu}\eta_{\rho\sigma} - 2\eta_{\mu\rho}\eta_{\nu\sigma}) \right] \\ \Rightarrow & \quad -i\frac{\kappa}{2} \{ [m_A^2 + (k_1 \cdot k_2)]C_{\mu\nu\rho\sigma} + D_{\mu\nu\rho\sigma}(k_1, k_2) \}, \end{aligned} \quad (2.22)$$

where we have symmetrized in $\mu \leftrightarrow \nu$ and assumed that all momenta are going into the vertex. In the second line, a factor of two was introduced, since we consider identical particles. This expression is also valid for coupling to non-abelian gauge fields, like gluons, provided we require identical color by introducing a Kronecker delta, δ^{ab} , in the vertex (see Appendix A). We will need both the abelian and non-abelian version, since we will consider diagrams with both graviton-photon-photon and graviton-gluon-gluon vertices.

2.2.3 Fermions

For fermion fields one has to use the vierbein (or tetrad) formalism. In this formalism, we use lower-case Latin indices, a, b, \dots , as the four Lorentz indices of Minkowski spacetime, whereas Greek indices, μ, ν, \dots , refer to general coordinates. Vierbeins, e_μ^a , have the following property, $e_\mu^a e_\nu^b \eta_{ab} = g_{\mu\nu}$, where we also define $e \equiv \det(e_\mu^a) \simeq 1 + \frac{\kappa}{2}(h + 4\phi)$, but the ϕ term is neglected here. Note also that $\sqrt{-g} = e$.

The Lagrangian density for a fermion field can be written

$$\mathcal{L}_F = \bar{\psi}(i\gamma^\mu \mathcal{D}_\mu - m_\psi)\psi, \quad (2.23)$$

where ψ is a fermion field, with the covariant derivative defined as

$$\mathcal{D}_\mu \psi = (D_\mu + \frac{1}{2}\omega_\mu^{ab}\sigma_{ab})\psi, \quad (2.24)$$

with D_μ defined in Eq. (2.13). Again we only consider the abelian case, hence the charge coefficient, Q , refers to fermion charge. For the spin connection, we use the definition [19]

$$\omega_{\mu ab} = \frac{1}{2}(\partial_\mu e_{b\nu} - \partial_\nu e_{b\mu})e_a^\nu - \frac{1}{2}(\partial_\mu e_{a\nu} - \partial_\nu e_{a\mu})e_b^\nu - \frac{1}{2}e_a^\rho e_b^\sigma (\partial_\rho e_{c\sigma} - \partial_\sigma e_{c\rho})e_\mu^c, \quad (2.25)$$

where σ_{ab} are 4×4 matrices, defined as $\sigma_{ab} = \frac{1}{4}[\gamma_a, \gamma_b]$.

In the case of fermions, the energy momentum tensor has a definition similar to the one in Eq. (2.9), but now with variation with respect to vierbeins instead of the metric tensor

$$T_{\mu\nu}^F \equiv \frac{1}{e} e_{\mu a} \frac{\delta(e\mathcal{L}_F)}{\delta e_a^\nu} = \left(-\eta_{\mu\nu} \mathcal{L}_F + e_{\mu a} \frac{\delta \mathcal{L}_F}{\delta e_a^\nu} \right) \Big|_{e=\delta}, \quad (2.26)$$

where we used the relation $\delta e = -e e_\mu^a \delta e_\mu^a$ and the linearized vierbein, $e_\mu^a = \delta_\mu^a - \frac{\kappa}{2} h_\mu^a$. The restriction $e = \delta$ means that each vierbein should be put equal to its respective Kronecker delta, to avoid terms of higher order in κ . However, this substitution should not be made immediately in the differentiated vierbeins involved in ω_μ^{ab} , since that would make this expression vanish. Before we substitute for those vierbeins, we use differentiation by parts, and the fact that total derivatives vanish upon integration.

The antisymmetry of σ_{ab} , together with the relation²

$$\gamma^a \gamma^b \gamma^c = \gamma^a \eta^{bc} - \gamma^b \eta^{ca} + \gamma^c \eta^{ab} - i\varepsilon^{abcd} \gamma_d \gamma_5, \quad (2.27)$$

²Here we use a convention where $\varepsilon_{0123} = +1$ and $\gamma_5 = i\gamma^0\gamma^1\gamma^2\gamma^3$.

and the fact that ε^{abcd} is antisymmetric in $a \leftrightarrow c$ is also needed to obtain the expression for the fermion energy momentum tensor

$$\begin{aligned} T_{\mu\nu}^F &= -\eta_{\mu\nu}(\bar{\psi}i\gamma^\rho D_\rho\psi - m_\psi\bar{\psi}\psi) + \frac{1}{2}\bar{\psi}i\gamma_\mu D_\nu\psi + \frac{1}{2}\bar{\psi}i\gamma_\nu D_\mu\psi \\ &\quad + \frac{1}{2}\eta_{\mu\nu}\partial^\rho(\bar{\psi}i\gamma_\rho\psi) - \frac{1}{4}\partial_\mu(\bar{\psi}i\gamma_\nu\psi) - \frac{1}{4}\partial_\nu(\bar{\psi}i\gamma_\mu\psi), \end{aligned} \quad (2.28)$$

where the second line comes from the term containing ω_μ^{ab} , and we have symmetrized in $\mu \leftrightarrow \nu$.

The interaction Lagrangian density for the KK gravitons becomes

$$\mathcal{L}_F^{\text{int}} = -\frac{\kappa}{2}[(h^{\mu\nu} - h\eta^{\mu\nu})\bar{\psi}i\gamma_\mu D_\nu\psi + m_\psi h\bar{\psi}\psi + \frac{1}{2}\bar{\psi}i\gamma^\mu(\partial^\nu h_{\mu\nu} - \partial_\mu h)\psi], \quad (2.29)$$

where we again used integration by parts. This Lagrangian describes the graviton-fermion-fermion and graviton-fermion-fermion-photon couplings.

From Eq. (2.29) we get the following 3-point vertex (graviton-fermion-fermion):

$$\begin{aligned} h^{\mu\nu}\bar{\psi}\psi : &\quad -i\frac{\kappa}{2}\left\{- (\eta_{\mu\nu}\eta_{\rho\sigma} - \eta_{\mu\rho}\eta_{\nu\sigma})h^{\mu\nu}\bar{\psi}i\gamma^\rho\partial^\sigma\psi + m_\psi\eta_{\mu\nu}h^{\mu\nu}\bar{\psi}\psi \right. \\ &\quad \left. - \frac{1}{2}\bar{\psi}i\gamma^\rho[(\partial_\rho h^{\mu\nu})\eta_{\mu\nu} - (\partial_\nu h^{\mu\nu})\eta_{\mu\rho}]\right\}\psi \\ \Rightarrow &\quad -i\frac{\kappa}{2}\left\{- (\eta_{\mu\nu}\eta_{\rho\sigma} - \eta_{\mu\rho}\eta_{\nu\sigma})i\gamma^\rho(-ik_1^\sigma) + m_\psi\eta_{\mu\nu} \right. \\ &\quad \left. - \frac{1}{2}i\gamma^\rho[(-ip_\rho)\eta_{\mu\nu} - (-ip_\nu)\eta_{\mu\rho}]\right\} \\ = &\quad -i\frac{\kappa}{2}\left[-\frac{1}{2}\eta_{\mu\nu}(\not{k}_1 + \not{k}_2 - 2m_\psi) + \frac{1}{2}(\gamma_\mu k_{1\nu} + \gamma_\nu k_{2\mu})\right] \\ = &\quad -i\frac{\kappa}{8}[\gamma_\mu(k_1 + k_2)_\nu + \gamma_\nu(k_1 + k_2)_\mu - 2\eta_{\mu\nu}(\not{k}_1 + \not{k}_2 - 2m_\psi)], \end{aligned} \quad (2.30)$$

where we have symmetrized the terms in $\mu \leftrightarrow \nu$ and used $-p = k_1 - k_2$, together with the notation $k = \gamma^\mu k_\mu$.

We also find a 4-point vertex (graviton-fermion-fermion-photon) from Eq. (2.29) with an additional gauge field

$$\begin{aligned} h^{\mu\nu}\bar{\psi}\psi A^\rho : &\quad -i\frac{\kappa}{2}h^{\mu\nu}[-(\eta_{\mu\nu}\eta_{\rho\sigma} - \eta_{\mu\sigma}\eta_{\nu\rho})\bar{\psi}i\gamma^\sigma(eQA^\rho)\psi] \\ \Rightarrow &\quad -i\frac{\kappa}{2}[-(\eta_{\mu\nu}\eta_{\rho\sigma} - \eta_{\mu\sigma}\eta_{\nu\rho})i\gamma^\sigma(eQ)] \\ = &\quad -i\frac{\kappa}{2}(eQ)\left[\frac{1}{2}\eta_{\mu\nu}\eta_{\rho\sigma} + \frac{1}{2}(\eta_{\mu\nu}\eta_{\rho\sigma} - \eta_{\mu\rho}\eta_{\nu\sigma} - \eta_{\mu\sigma}\eta_{\nu\rho})\right]\gamma^\sigma \\ = &\quad i\frac{\kappa}{4}(eQ)[C_{\mu\nu\rho\sigma} - \eta_{\mu\nu}\eta_{\rho\sigma}]\gamma^\sigma, \end{aligned} \quad (2.31)$$

where we have symmetrized the terms in $\mu \leftrightarrow \nu$. In order to obtain the corresponding expression for non-abelian fields, we substitute $eQ \rightarrow gT^a$.

Several other vertices where gravitons are involved are given in [19] but since we do not need them we will not derive them here, although it is straightforward.

2.2.4 The Graviton Propagator

In addition to the vertex rules derived in the previous section, we also need the massive graviton propagator, which will not be derived here. This propagator can be expressed as [21]³

$$i\Delta_{\mu\nu\rho\sigma}^{\bar{n}} = \frac{iP_{\mu\nu\rho\sigma}}{k^2 - m_{\bar{n}}^2 + i\varepsilon}, \quad (2.32)$$

with

$$P_{\mu\nu\rho\sigma} = \eta_{\mu\rho}\eta_{\nu\sigma} + \eta_{\mu\sigma}\eta_{\nu\rho} - \frac{2}{3}\eta_{\mu\nu}\eta_{\rho\sigma}, \quad (2.33)$$

where we have neglected terms that are quadratic and quartic in the transferred momenta since such terms vanish upon coupling to a conserved current. The corresponding massless graviton propagator is obtained by substituting $P_{\mu\nu\rho\sigma} \rightarrow C_{\mu\nu\rho\sigma}$. Note that in the limit $m_{\bar{n}} \rightarrow 0$, the massive propagator is different from the massless propagator. This is the so-called van Dam–Veltman–Zakharov discontinuity [21], which gives different results for massive and massless gravitons for e.g. the bending of light. The predictions have been tested experimentally, and the massive case has been ruled out. This does not mean that massive gravitons cannot exist, it only means that at large distances, the properties of gravity, as we know it, are determined by the existence of a massless graviton. However, in the context of extra-dimensional theories, massive gravitons can exist in addition to the massless graviton.

A summary of the Feynman rules given in this chapter is presented in Appendix A. For SM Feynman rules, see e.g. [22].

³Here we use the normalization of [19], which differs from the one used in [21].

Chapter 3

Phenomenology of Extra-Dimensional Scenarios

In this chapter we shall describe a few selected scenarios of extra dimensions and their phenomenology. Since the papers I–IV focus on the Arkani-Hamed–Dimopoulos–Dvali (ADD) and the Randall–Sundrum (RS) scenarios, those two will be discussed in detail. However, in Sect. 3.3, we will also briefly mention some of the alternative scenarios. This is not meant to be a comprehensive review, with all relevant references included, but instead we will mention some of the features of these models and quote a few relevant references (see e.g. [20, 23, 24, 25, 26, 27] for more complete reviews).

3.1 Arkani-Hamed–Dimopoulos–Dvali Scenario

In 1998, Arkani-Hamed, Dimopoulos and Dvali suggested that there could exist yet undiscovered extra space dimensions at the mm scale [12]. This suggestion, known as the ADD scenario, triggered an enormous activity in the field of extra dimensions in the years to come, which have generated thousands of citations to the original paper.

The motivation for introducing these extra dimensions was to offer an alternative framework for solving the *hierarchy problem*. This problem is related to the weakness of gravity compared to the other forces in nature. The question is why the electroweak scale and the Planck scale are so different. Explaining this problem without fine-tuning has turned out to be a very challenging task. Furthermore, a scalar field, like the Higgs, would get corrections to its mass of the order of the Planck scale, and therefore it is difficult to obtain a cancellation of such corrections to give the Higgs a mass of only $\mathcal{O}(100 \text{ GeV})$.

It should also be mentioned that the hierarchy problem is not completely solved in the ADD scenario, since a new, but milder, hierarchy between the compactification scale, $\mu_c \sim 1/R$, and the electroweak scale is introduced. Moreover, the hierarchy problem may also be solved in theories involving technicolor or supersymmetry.

At the time when this scenario was proposed, the gravitational force had only been measured down to distances $\mathcal{O}(1 \text{ cm})$ [28]. An extrapolation over 33 orders of magni-

tude, based on the assumption that gravity is unmodified, is required to get from the experimentally measured range to the Planck scale. State-of-the-art table top experiments have been able to test gravity at shorter distances, and thereby push the upper limit of the compactification radius down to $150 \mu\text{m}$ [13], but still an enormous untested range remains.

The philosophy of the ADD scenario is that there is only one fundamental scale in nature, namely the electroweak scale, m_{EW} . Hence, the hierarchy is removed by lowering the Planck scale. The apparent weakness of gravity and the gigantic Planck scale is due to the existence of extra space dimensions in which only gravity can propagate. If this is the case, gravity should obey a $1/r^{2+n}$ law instead of the famous $1/r^2$ law. However, if the extra dimensions are compactified, with compactification radii R less than $\mathcal{O}(1 \text{ mm})$, they could have escaped observation.

At large distances, where space-time effectively is four-dimensional, we have the familiar Newton's force law [see also Eq. (1.1)]

$$F_g(r) \sim \frac{m_1 m_2}{M_{\text{Pl}}^2 r^2}, \quad r \gg R. \quad (3.1)$$

According to the ADD scenario, there are n extra space dimensions, which at short distances lead to the following force law

$$F_g(r) \sim \frac{m_1 m_2}{M_D^{n+2} r^{n+2}}, \quad r \ll R, \quad (3.2)$$

where M_D is the fundamental Planck scale of the higher dimensional theory, which is required to be $\mathcal{O}(m_{EW})$. Matching these expressions at distance R gives the relation

$$M_{\text{Pl}}^2 \sim M_D^{n+2} R^n. \quad (3.3)$$

For a given number of extra dimensions, n , the compactification radius, R , can be chosen to reproduce the conventional M_{Pl} . For $n = 1$, this exercise leads to $R \sim 10^{13} \text{ cm}$, which is comparable to the earth-moon distance. Obviously this case is ruled out, but already at $n = 2$, the required compactification radius is of the order of the exclusion limit from table-top experiments. For $n > 2$, such experiments will have difficulties excluding the ADD model. The reason why table-top experiments cannot lower the exclusion limits significantly is that they would enter the regime of van der Waal forces.

The fact that the compactification radius, R , in the ADD model decreases significantly if the number of extra dimensions is increased can be seen from the expression [29]

$$R_n = 2 \times 10^{\frac{31}{n}-16} \text{ mm} \times \left(\frac{1 \text{ TeV}}{M_D} \right)^{1+\frac{2}{n}}. \quad (3.4)$$

For $n = 6$ and $M_D = 1 \text{ TeV}$, we find that R_6 is $\mathcal{O}(10^{-11} \text{ mm})$, which is very different from the corresponding value for $n = 2$.

Although these numbers may seem small, they are not small in the world of particle physics, where the resolution in typical experiments is $\mathcal{O}(10^{-15} \text{ mm})$. Therefore, the models

based on the ADD scenario are often referred to as theories of “Large Extra Dimensions” (LED).

Since gravity seems so weak compared to the other known forces of nature, it has usually been neglected in particle physics experiments. In the ADD model, every single KK graviton only interacts with gravitational couplings to the SM particles. However, the fact that they are so numerous leads to the possibility of observing graviton effects in particle physics experiments, something which would be an indication of extra dimensions. Current and planned experiments are able to constrain the limits on extra dimensions even further than the table-top experiments, or even discover extra dimensions if such exist. In Sects. 3.4 and 3.5, we will comment more on existing bounds, together with the experimental reach in upcoming collider searches.

When it comes to collider searches for extra dimensions, there are two different classes of signals. One possibility is to look for missing energy in the particle collisions. This would be due to production of KK gravitons which escape from our four-dimensional world into the extra dimensions. In order to produce such real gravitons, their mass cannot be above the collision energy. Another possibility is that exchange of virtual KK gravitons will lead to an enhancement of events of different signatures. The latter case results in an infinite sum over all the KK modes, where an ultraviolet (UV) cut-off is introduced to avoid divergences. There is therefore an important difference between these two approaches, since one is directly sensitive to the fundamental Planck scale, whereas in the other, the UV cut-off enters.

3.1.1 Summation over KK Modes

In the ADD scenario, where the mass splittings in the KK tower are tiny because of the large compactification size, there will to a good approximation be a continuum of states. Therefore, the summation over the KK modes can be approximated by an integral.

Due to the fact that three similar papers appeared almost simultaneously [18, 19, 30], there is still some different notation around when it comes to summing over the KK tower. We shall here refer to these different notations as Giudice–Rattazzi–Wells (GRW), Han–Lykken–Zhang (HLZ) and Hewett.

Note that we do not use the same notation in all four papers. In Papers I–III on graviton-induced bremsstrahlung, we used the HLZ notation, since in this notation the exchanged momentum is explicit. This is convenient when it comes to distinguishing between initial- and final-state radiation. In Paper IV on center–edge asymmetry at hadron colliders, the notation of Hewett was used, since we wanted to keep the notation which was used in the e^+e^- collider paper on the same subject [31].

HLZ Notation

The approach followed by Han et al. [19] is to substitute the following expression for the sum over propagators

$$-i\kappa^2 D(s) \equiv \sum_{\bar{n}} \frac{\kappa^2}{s - m_{\bar{n}}^2 + i\varepsilon} \rightarrow \int_0^\infty dm_{\bar{n}}^2 \rho(m_{\bar{n}}) \frac{\kappa^2}{s - m_{\bar{n}}^2 + i\varepsilon}, \quad (3.5)$$

where the density of states can be expressed as¹

$$\rho(m_{\bar{n}}) = \frac{R^n m_{\bar{n}}^{n-2}}{(4\pi)^{n/2} \Gamma(n/2)}. \quad (3.6)$$

If we now use the formula

$$\frac{1}{s - m_{\bar{n}}^2 + i\varepsilon} = P \left(\frac{1}{s - m_{\bar{n}}^2} \right) - i\pi \delta(s - m_{\bar{n}}^2), \quad (3.7)$$

the principal value of the integral in Eq. (3.5) can be evaluated by substituting $m/\sqrt{s} \rightarrow y$ and introducing an UV cut-off, $x = M_S/\sqrt{s}$, to avoid divergences. Presumably, M_S is of the same magnitude as the higher-dimensional Planck mass, M_D . If we adopt the definition of the relationship between the UV cut-off, M_S , the compactification scale, R and the gravitational coupling, $\kappa = \sqrt{16\pi}/M_{\text{Pl}}$, given in [19]

$$\kappa^2 R^n = 8\pi(4\pi)^{n/2} \Gamma(n/2) M_S^{-(n+2)}, \quad (3.8)$$

we can express $D(s)$ as

$$-i\kappa^2 D(s) = \frac{8\pi s^{n/2-1}}{M_S^{n+2}} [2I(x) - i\pi], \quad (3.9)$$

where

$$I(x) = P \int_0^x dy \frac{y^{n-1}}{1-y^2}. \quad (3.10)$$

When performing the integral, $I(x)$, it is convenient to consider even and odd values of n separately. For n even, we have

$$\begin{aligned} I(x) &= - \sum_{k=1}^{n/2-1} \int_0^x dy y^{2k-1} + P \int_0^x dy \frac{y}{1-y^2} \\ &= - \sum_{k=1}^{n/2-1} \frac{1}{2k} x^{2k} - \frac{1}{2} \log(x^2 - 1), \end{aligned} \quad (3.11)$$

¹The compactification radius is $R/2\pi$ in the HLZ notation.

whereas for n odd we get

$$\begin{aligned} I(x) &= - \sum_{k=1}^{(n-1)/2} \int_0^x dy y^{2k-2} + P \int_0^x dy \frac{1}{1-y^2} \\ &= - \sum_{k=1}^{(n-1)/2} \frac{1}{2k-1} x^{2k-1} + \frac{1}{2} \log \left(\frac{x+1}{x-1} \right). \end{aligned} \quad (3.12)$$

Note that this approach is sensitive to the number of extra dimensions, n .

In order to compare with other notations, we consider the limit $\sqrt{s} \ll M_S$ of Eq. (3.9), where

$$-i\kappa^2 D(s) = -i8\pi C_4 \simeq \begin{cases} -\frac{8\pi}{M_S^4} \log \left(\frac{M_S^2}{s} \right), & n = 2, \\ -\frac{16\pi}{(n-2)M_S^4} & n > 2. \end{cases} \quad (3.13)$$

GRW Notation

Giudice et al. [18] follow an approach which is similar to the one described above, and therefore we do not go into detail here. They also approximate the sum over KK modes by an integral and end up with the following expression

$$-i\kappa^2 D(s) = -\frac{8\pi}{\Lambda_T^4}, \quad n > 2, \quad (3.14)$$

where the UV cut-off, Λ_T , depends on the number of extra dimensions in addition to unknown coefficients. According to [18], these coefficients are not computable in the effective theory, but are assumed to be of the order of the higher-dimensional Planck mass, M_D .

Note that if we compare the approximation in Eq. (3.13) to the one in Eq. (3.14), we get the relation

$$M_S|_{n=4} = \Lambda_T. \quad (3.15)$$

Hewett Notation

In the Hewett approach [30], the details of how to perform the sum over KK modes is not explained in detail in the original paper. However, this approach is very similar to GRW, and it is also stated that the exact computation of the integral can only be performed with some knowledge of the full underlying theory. Hewett uses the notation

$$-i\kappa^2 D(s) = -\frac{16\lambda}{M_H^4}, \quad (3.16)$$

where M_H is the UV cut-off, and λ depends on the number of extra dimensions, but is assumed to be $\mathcal{O}(1)$. However, the sign, which determines whether we have constructive or destructive interference, is unknown. This parameter is usually interpreted as a sign factor, $\lambda = \pm 1$ in phenomenological considerations.

If we compare this notation to the two others, we find

$$M_S|_{n=4} = \Lambda_T = \sqrt[4]{\frac{\pi}{2}} M_H|_{\lambda=+1}. \quad (3.17)$$

3.2 Randall–Sundrum Scenario

In this section we will describe the Randall–Sundrum scenario [32], which is an alternative approach to the hierarchy problem, quite distinct from the ADD scenario. Actually, Randall and Sundrum proposed two different scenarios, often referred to as RS I and RS II. In this thesis we shall mainly be concerned with the RS I scenario, and for simplicity only refer to it as the RS scenario. The RS II scenario will be discussed briefly in the next section.

The RS scenario is a five-dimensional scenario, but unlike the ADD scenario, the case of one extra space dimension is not ruled out by experiments. The fifth dimension, which is periodic, can be parametrized by θ , where $-\pi \leq \theta \leq \pi$ and with the additional constraint that (x, θ) is identified with $(x, -\theta)$, where x represents the four-dimensional coordinates. This construction, which is referred to as an S_1/\mathbf{Z}_2 orbifold, has two fixed points, $\theta = 0$ and $\theta = \pi$. At each of these fixed points, there is a 3-brane, and we live on one of them, whereas the other one is hidden for us. Between the two 3-branes is a slice of Anti-de-Sitter space, AdS_5 , and for the scenario considered here, only gravity is allowed to propagate in the extra space-dimension.

In the RS scenario, the metric is assumed to be non-factorizable, meaning that the four-dimensional metric is a function of the coordinate of the fifth dimension. It can be expressed as

$$ds^2 = e^{-2kr_c|\theta|} \eta_{\mu\nu} dx^\mu dx^\nu + r_c^2 d\theta^2, \quad (3.18)$$

where k , which is related to the curvature of the AdS_5 space, is of the order of the Planck scale and r_c is the compactification radius. The exponential factor is often referred to as a “warp” factor, hence theories related to the RS scenario are often referred to as theories of “warped extra dimensions”.

Randall and Sundrum solved the five-dimensional Einstein equations in this model and derived the following expressions for the brane tensions, V_{hidden} and V_{visible} , and the cosmological constant, Λ , [32]

$$\begin{aligned} V_{\text{hidden}} &= 24M_5^3 k = -V_{\text{visible}}, \\ \Lambda &= -24M_5^3 k^2, \end{aligned} \quad (3.19)$$

where M_5 is the fundamental Planck mass in the higher dimensional theory. These two fine-tuning conditions can be related to radius stabilization and vanishing of the $4D$ cosmological constant [20]. The relation between the four-dimensional Planck mass, M_{Pl} and the fundamental Planck mass, M_5 can also be derived in this model, and the result is

$$M_{\text{Pl}}^2 = \frac{M_5^3}{k} [1 - e^{-2kr_c\pi}]. \quad (3.20)$$

Note that this result depends only weakly on the compactification radius when kr_c is large.

The warp factor is more important when it comes to determining the physical masses on the visible 3-brane. A mass parameter, m_0 , in the higher-dimensional theory corresponds to a physical mass

$$m \equiv e^{-kr_c\pi} m_0. \quad (3.21)$$

To obtain TeV-scale physics from fundamental mass parameters not far from the Planck scale, $kr_c \simeq 12$ is sufficient. Hence, no large mass hierarchy between the fundamental parameters is generated. An alternative viewpoint (technically established through a change of coordinates), which would be natural for a four-dimensional observer is that the TeV scale is the fundamental scale, whereas the Planck scale is the derived scale².

The phenomenology of the RS scenario is rather different from the ADD scenario. Again there will be a tower of KK graviton resonances, but now with masses at the TeV scale and TeV scale suppressed rather than Planck scale suppressed couplings to SM particles. This results in the possibility of detecting each mode individually in particle collider experiments, provided they are in the accessible range.

In the RS scenario, the masses of the KK gravitons are given by [33],

$$m_n = k x_n e^{-kr_c\pi} = m_1 \frac{x_n}{x_1}, \quad (3.22)$$

where x_i are the roots of J_1 , the first order Bessel function. The first roots [34] are given in Table 3.1 (see also Fig. III-10).

Table 3.1: Roots of the Bessel function $J_1(x_i) = 0$.

$x_1 = 3.83171$	$x_5 = 16.47063$	$x_9 = 29.04683$
$x_2 = 7.01559$	$x_6 = 19.61586$	$x_{10} = 32.18968$
$x_3 = 10.17347$	$x_7 = 22.76008$	$x_{11} = 35.33231$
$x_4 = 13.32369$	$x_8 = 25.90367$	$x_{12} = 38.47477$

Note that since the mass of the first graviton resonance is expected to be in the TeV range, the mass splittings will also be of the order of TeV. Thus only a few KK gravitons will be in the accessible range of particle colliders, and the infinite sum can be truncated after only a few terms.

In the RS model, the action describing the interaction between gravitons and matter can be expressed as [33]

$$\mathcal{S}_{\text{RS}} = -\frac{1}{2} \int d^4x \left[\frac{\sqrt{2}}{\overline{M}_{\text{Pl}}} T^{\mu\nu} h_{\mu\nu}^{(0)} + \frac{\sqrt{2}}{\Lambda_\pi} T^{\mu\nu} \sum_{n=1}^{\infty} h_{\mu\nu}^{(n)} \right], \quad (3.23)$$

²The only small number in this setup is the small overlap of the graviton wave function in the fifth dimension with our brane.

where we introduced the factor of $1/\sqrt{2}$ to be in agreement with our normalization of the graviton propagator. The first term in Eq. (3.23) is the coupling of the massless graviton, which is suppressed by the Planck mass. The second term is suppressed by Λ_π , which describes the coupling between massive KK gravitons and matter, where [33]

$$\Lambda_\pi = e^{-kr_c\pi} \overline{M}_{\text{Pl}} = \frac{m_1 \overline{M}_{\text{Pl}}}{x_1 k}, \quad (3.24)$$

and is therefore only TeV suppressed. As seen from Eqs. (3.22) and (3.24), the graviton sector of the RS scenario is completely determined by the two parameters m_1 and $k/\overline{M}_{\text{Pl}}$. The dimensionless parameter, $k/\overline{M}_{\text{Pl}}$, determines the coupling strength of the KK gravitons, and is expected to be between 0.01 and 0.1 [33].

There is also a scalar particle in this model, often referred to as the radion, which couples to the trace of the energy-momentum tensor. If this particle is lighter than the first KK excitation, which could very well be the case, it may provide the first hint in the direction of the RS model. Due to Higgs-radion mixing, the properties of the SM Higgs may be affected [35]. However, we do not consider the RS radion in this thesis.

If we now compare the massive graviton coupling of Eqs. (2.10) and (3.23), we find that

$$\kappa = \sqrt{2} \frac{x_1}{m_1} \left(\frac{k}{\overline{M}_{\text{Pl}}} \right). \quad (3.25)$$

Hence, if we modify the definition of κ given in Sect. 1.2 according to Eq. (3.25), we can use the results derived in the previous chapter also for the RS gravitons.

Using the Feynman rules of Chapt. 2, we can obtain the decay rate of e.g. graviton decay into two photons

$$\Gamma(G \rightarrow \gamma\gamma) = \frac{x_n^2 m_n}{80\pi} \left(\frac{k}{\overline{M}_{\text{Pl}}} \right)^2. \quad (3.26)$$

Similar expressions, for decay to other SM particles (in the massless limit), are given in Eqs. (II-5.5)–(II-5.7). The reason for calculating the decay rates to SM particles is to obtain the total width, which enters in the cross section calculations through the graviton propagator.

3.3 Alternative Scenarios

As stated above, there exists an enormous number of theories involving extra dimensions with various shapes and sizes, a few of which will be mentioned here.

One of the alternatives is the model by Dienes, Dudas and Gherghetta, which in contrast to the ADD and RS models allows for SM fields to propagate in extra dimensions [36], something which would lead to KK excitations of the SM particles³. Therefore, the constraints from collider experiments are much more stringent in this case, hence such

³Actually, they consider the Minimal Supersymmetric Standard Model (MSSM).

extra dimensions must have a compactification radius $R \lesssim 10^{-19}$ m. In this model, the Yukawa couplings would receive power-law corrections, which could lead to unified theories at scales much below the usual GUT scale.

In addition to the model described in Sect. 3.2, Randall and Sundrum also proposed a model with an infinite extra dimension, referred to as RS II [37]. In this model, the graviton is localized to our brane, such that known tests of gravity are not violated. There are also alternative versions of the RS scenarios, with some or all SM fields in the bulk [38], more than one warped extra dimension [39], multibrane constructions [40] and intersecting branes [41].

The cosmology of brane world scenarios has also been studied [42], and even scenarios for an ekpyrotic universe [43] with colliding branes have been proposed as alternatives to the Big Bang theory.

Models where all the SM fields are in the bulk are often referred to as Universal Extra Dimensions (UED) [44]. In such models there are no walls present, and the KK number is conserved at tree-level due to translational invariance and momentum conservation in the higher dimensions. This leads to the possibility of pair production of KK states, with the lowest KK state (of the light quarks and gluons) being stable.

There are also models which try to explain the tiny neutrino masses by putting right-handed neutrinos in the bulk [45]. If there are SM fields propagating in extra dimensions, they do not necessarily propagate in the same number of dimensions as gravity.

The shape of extra dimensions is in most cases for simplicity assumed to be circular or toroidal, but different options have also been considered, with notions such as “football shaped” extra dimensions⁴ [46].

Arkani-Hamed et al. have also suggested a way to (de)construct extra dimensions [47]. Their theory is four-dimensional at very high energies, but at lower energies, extra dimensions emerge dynamically.

Here we have presented some of the extra-dimensional theories available. There are several other alternatives, but as indicated above, to give a complete overview is far beyond the scope of this thesis.

3.4 Collider Phenomenology

If extra dimensions are realized in nature, there is a huge number of possible experimental signatures. Although the signatures may be model dependent, search strategies which will be sensitive to a large fraction of the suggested signals have been proposed. Some of the models have signatures which are similar to those of models beyond the SM without extra dimensions, whereas other signatures would clearly be evidence that extra dimensions are at work.

As mentioned in Sect. 3.1, both direct production and virtual exchange of KK gravitons offer possible signals when it comes to collider searches for extra dimensions. Here we shall

⁴Referring to American footballs.

review briefly some of the signals relevant for collider searches. We will mention past (LEP), present (HERA, Tevatron) and future (LHC, TESLA, CLIC) experiments.

- LEP: e^+e^- collider with 200 GeV c.m. energy, finished in 2000.
- HERA: ep collider with 319 GeV c.m. energy. Can run in both e^+ and e^- mode.
- Tevatron: $p\bar{p}$ collider with 1.8 TeV c.m. energy (Run I), which has been upgraded to 1.96 TeV (Run II) and is currently taking data.
- LHC: pp collider with 14 TeV c.m. energy, which is currently under construction, and is scheduled to start up in 2007.
- TESLA: A proposed 0.5–1 TeV linear e^+e^- collider.
- CLIC: A proposed 3–5 TeV linear e^+e^- collider.

The possibility of running a future e^+e^- collider in $\gamma\gamma$ mode is also being investigated.

In the ADD case, a typical experimental signature of direct graviton production will be missing transverse energy, \cancel{E}_T . The reason for this is that the KK gravitons are very long-lived and can therefore escape detection. At hadron colliders, processes such as

$$\begin{aligned} pp &\rightarrow \text{jet} + \cancel{E}_T, \\ pp &\rightarrow \gamma + \cancel{E}_T, \end{aligned} \tag{3.27}$$

can be used to search for extra dimensions [18]. The dominant subprocess to the jet + \cancel{E}_T channel is $qg \rightarrow qG$, where the graviton, G , would escape into the extra dimensions and thus lead to missing energy. Standard Model processes can also contribute, and the dominant background to the missing energy in such processes is $Z \rightarrow \nu\bar{\nu}$.

The processes in Eq. (3.27) are sensitive to both the fundamental Planck scale, M_D , and the number of extra dimensions. At the LHC, with an integrated luminosity of $\mathcal{L} = 100 \text{ fb}^{-1}$, the maximum M_D sensitivity given in [18] for the jet + \cancel{E}_T channel is in the range 8.5–5 TeV for n between 2 and 5. For the $\gamma + \cancel{E}_T$ channel, a reach of 4.5 TeV is expected ($n = 2$) [48].

The Tevatron (D0) results for the jet + \cancel{E}_T channel are M_D reach in the range 1.0–0.6 TeV for n between 2 and 7 [49]. By analyzing $\gamma + \cancel{E}_T$ data collected at the CDF detector at the Tevatron (Run I), exclusion limits on M_D in the range 600–550 GeV have been found for n between 4 and 8 [50]. This final state has also been analyzed at LEP, which reaches limits in the M_D range 1.31–0.58 TeV for n between 2 and 6 [51]. According to preliminary LEP results presented at the ICHEP'04 conference held in Beijing, August 2004, these bounds have now increased to 1.60–0.66 TeV.

Also the process $pp \rightarrow l^+l^- + \cancel{E}_T + X$ which can proceed through 14 diagrams has been studied for the LHC case [52] (see also [53]), and the signal is expected to have a harder \cancel{E}_T spectrum than the corresponding background. The reach on M_D is 4 TeV for $n = 3$ in this channel, which is lower than for the $\gamma + \cancel{E}_T$ channel since there is one more particle

in the final state. An analogous study at e^+e^- colliders has also been carried out [54]. At 500 GeV with $\mathcal{L} = 500 \text{ fb}^{-1}$, the M_D reach would be 4.1–1.1 TeV for $n = 2-7$.

The results based on real graviton emission mentioned above are summarized in Table 3.2.

Table 3.2: Summary of the existing and expected bounds from real graviton emission. Existing bounds have collider names in boldface.

Collider	Final state	M_D [TeV]	n	Reference
LEP	$\gamma + \cancel{E}_T$	1.31–0.58	2–6	[51]
LEP	$\gamma + \cancel{E}_T$	1.60–0.66	2–6	ICHEP'04
Tevatron	$\gamma + \cancel{E}_T$	0.6–0.55	4–8	[50]
LHC	$\gamma + \cancel{E}_T$	4.5	2	[48]
Tevatron	jet + \cancel{E}_T	1.0–0.6	2–7	[49]
LHC	jet + \cancel{E}_T	8.5–5	2–7	[18]
LHC	$l^+l^- + \cancel{E}_T$	4	3	[52]
TESLA	$l^+l^- + \cancel{E}_T$	4.1–1.1	2–7	[54]

When it comes to virtual exchange of KK gravitons, a typical signature at colliders is pair production of SM particles with a rate different from the SM prediction. Exchange of KK gravitons opens up new channels, described by subprocesses like

$$\begin{aligned}
 gg &\rightarrow G \rightarrow l^+l^-, \\
 q\bar{q} &\rightarrow G \rightarrow \gamma\gamma.
 \end{aligned}
 \tag{3.28}$$

Another example is given in the Feynman diagram of Fig. 3.1, with an electron-positron pair in the final state. At hadron colliders, the dijet final state has a higher background, and is therefore a more challenging channel. The same final states are also available at e^+e^- colliders.

There are several papers investigating virtual exchange within the ADD model. However, the notation may vary from paper to paper and therefore it is not always straightforward to compare the results. In [30], the dilepton channel is considered at the LHC, where the expected reach on M_H is 6 TeV ($\lambda = \pm 1$). The forward-backward asymmetry at both the Tevatron and the LHC is also considered. Such additional channels will in the ADD model contribute to a rather smooth increase in the cross section.

The diphoton signal, which is a very clean signal at hadron colliders, has been studied in [18], where a reach on Λ_T up to 7.1 TeV is given for the LHC case. In [55], the same channel is studied, but with results given in a different notation as a reach on M_S of 6.7–3 TeV for $n = 3-7$. Furthermore, the pseudorapidity distribution is presented. The cut $M_{\gamma\gamma} < 0.9M_S$ is introduced when integrating over the diphoton invariant mass, $M_{\gamma\gamma}$, not to conflict with

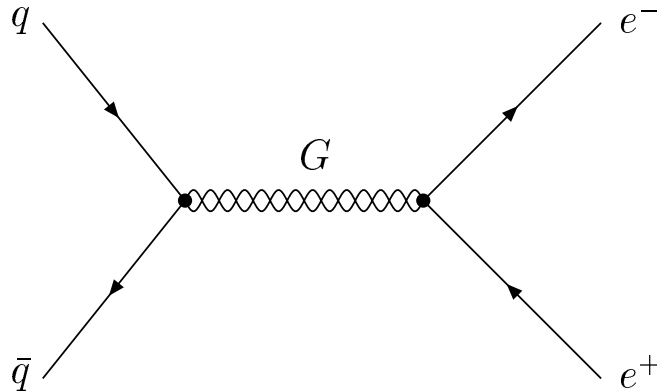


Figure 3.1: Feynman diagram with graviton exchange for the subprocess $q\bar{q} \rightarrow G \rightarrow e^+e^-$.

unitarity. Moreover, in [55], the SM box diagrams for $gg \rightarrow \gamma\gamma$, which interfere with the tree-level graviton exchange process, are included. However, at tree-level, there is still the SM background from $q\bar{q} \rightarrow \gamma\gamma$. The diphoton channel has also been investigated at the Tevatron (Run II), where the M_S reach of 1.9–1.5 TeV is found for $n = 3-7$ [55].

Also in the case of e^+e^- and $\gamma\gamma$ colliders the diphoton signal has been studied [56]. In particular the $\gamma\gamma \rightarrow \gamma\gamma$ process is interesting, since there is no tree-level process in the SM. At e^+e^- colliders, the reach on M_S is given as 3.5–5.5 times \sqrt{s} for a 5% deviation from the SM prediction, whereas the corresponding $\gamma\gamma$ collider numbers are 5–8 times \sqrt{s} . Combined measurements at LEP for the cross section and the forward-backward asymmetry in $f\bar{f}$ final-states yield lower bounds on M_H at 1.2 ($\lambda = +1$) and 1.1 TeV ($\lambda = -1$) [57].

The double differential cross section in the invariant mass and scattering angle is, according to [58] a powerful strategy for detecting gravity effects. The dilepton and diphoton channels (combined) are considered, with a 3.5–2.1 TeV reach on M_S at the Tevatron (Run II), and a 12.8–7.9 TeV reach at the LHC for $n = 2-7$. Here, the unitarity constraint of [55] is not taken into account, something which partly accounts for the higher reach.

By using the approach of double differential cross sections in dielectron and diphoton production on the Tevatron (Run I) results, a reach on M_S of 1.4–1 TeV is obtained for $n = 2-7$, with the corresponding limits on M_H being 1.1 and 1 TeV for $\lambda = \pm 1$ [59]. The latest (preliminary) M_S bounds, presented at the ICHEP'04 conference, are 1.67–1.14 TeV.

In [60], the dijet production at hadron colliders is considered. Testing of many experimental observables is performed in order to find those which give the highest reach on M_S . The search reach reported for the p_\perp distribution is $M_S = 3.1$ TeV at the Tevatron, and 20.8 TeV at the LHC for $n = 3$. Also the p_\perp^2 and τ distributions give comparable limits⁵.

⁵Here, τ is the product of parton momentum fractions.

Final states such as Higgs pair production [61], ZZ and W^+W^- production [62] (at e^+e^- colliders) and $t\bar{t}$ production [63] (at the Tevatron and LHC) have also been considered, but these studies will not be commented on here.

At the ep collisions at HERA, searches for virtual graviton exchange in the t -channel have resulted in (preliminary) bounds on M_H of the order of 0.8 TeV presented at the ICHEP'04 conference. However, the underlying processes are not relevant to the content of the papers in this thesis, thus we will not discuss these bounds.

In Table 3.3 we give a summary of the results from virtual graviton emission mentioned above.

Table 3.3: Summary of the existing and expected bounds from virtual graviton emission. Existing bounds have collider names in boldface.

Collider	Final state	M_S, Λ_T, M_H [TeV]	n, λ	Reference
LEP	$f\bar{f}$	1.2–1.1	$\lambda = +1, -1$	[57]
Tevatron	$\gamma\gamma$	1.9–1.5	3–7	[55]
LHC	$\gamma\gamma$	7.1		[18]
LHC	$\gamma\gamma$	6.7–3	3–7	[55]
TESLA	$\gamma\gamma$	$3.5\text{--}5.5 \times \sqrt{s}$		[56]
TESLA ($\gamma\gamma$)	$\gamma\gamma$	$5\text{--}8 \times \sqrt{s}$		[56]
LHC	l^+l^-	6	$\lambda = \pm 1$	[30]
Tevatron	l^+l^- and $\gamma\gamma$	1.4–1	2–7	[59]
Tevatron	l^+l^- and $\gamma\gamma$	1.67–1.14	2–7	ICHEP'04
Tevatron	l^+l^- and $\gamma\gamma$	3.5–2.1	2–7	[58]
LHC	l^+l^- and $\gamma\gamma$	12.8–7.9	2–7	[58]
Tevatron	dijet	3.1	3	[60]
LHC	dijet	20.8	3	[60]

In contrast to the ADD scenario, the KK gravitons in the RS scenario are very short-lived, and will normally decay inside the detector [64]. This will result in sharp peaks in the cross section as opposed to the smooth ADD cross section. For an illustration of this difference, see e.g. Figs. II-3 and II-5.

The two-body branching fractions for the first KK resonance into SM particles are given in [33] as functions of m_1 . The dijet final states dominate, whereas the cleaner dilepton channel has a branching fraction of a few percent. Furthermore, the allowed parameter space is presented, where both theoretical and experimental bounds are taken into account.

Detailed detector simulation studies at both the CMS [65] and ATLAS experiments [66] (LHC) have demonstrated that the RS scenario can be completely excluded at the LHC through dilepton and diphoton final states. Preliminary exclusion bounds from the

Tevatron, presented at the ICHEP'04 conference, are 300–785 GeV for the mass of the first resonance, m_1 (for k/\bar{M}_{Pl} between 0.01 and 0.1).

Although several theories beyond the SM can mimic each other's signals, the angular distribution arising from the exchange of a spin-2 particle like the graviton is very special, with quartic terms in the cosine of the scattering angle, compared to the quadratic terms of spin-1 exchange. Therefore, determining the spin of the exchanged particle in such processes will be crucial.

In [66], an extensive study of different two-body final-states in the RS model is carried out. Moreover, the angular distribution for the (sub)processes with two-body final states are given. The angular distributions in the massless fermion limit are given in Table 3.4, where f stands for fermion, and θ is the c.m. scattering angle. Note that these expressions are valid in both the ADD and RS model. In addition, spin-1 exchange produces the familiar $1 + \cos^2 \theta$ distribution, whereas spin-0 exchange gives a flat angular distribution.

Table 3.4: Angular distributions for graviton exchange.

Process	Angular distribution
$\gamma\gamma, gg \rightarrow G \rightarrow f\bar{f}$	$1 - \cos^4 \theta$
$f\bar{f} \rightarrow G \rightarrow \gamma\gamma, gg$	$1 - \cos^4 \theta$
$\gamma\gamma, gg \rightarrow G \rightarrow \gamma\gamma, gg$	$1 + 6 \cos^2 \theta + \cos^4 \theta$
$f\bar{f} \rightarrow G \rightarrow f\bar{f}$	$1 - 3 \cos^2 \theta + 4 \cos^4 \theta$

The possibility of determining the spin-2 of the RS graviton by a fit to the angular distribution has been investigated through CMS detector simulation studies [65]. For $k/\bar{M}_{\text{Pl}} = 0.1$, they report a reach in m_1 up to 2.4 TeV for dilepton final states.

Alternative approaches for spin determination, using moments of the (normalized) cross section for the angular distribution with respect to Legendre polynomials [67] and the center-edge asymmetry [31] have also been suggested. As a complementary signature of the angular distribution, the p_\perp spectrum is in [68] used to probe the characteristic mixture of gg and $q\bar{q}$ initial states in dilepton production within the RS scenario.

There are also papers treating the topics of graviscalar and radion searches [35, 69, 70]. Furthermore, the possibility of KK excitations of SM particles has been studied (see e.g. [33]), but we will not go into detail on these subjects.

Finally, we shall only mention that one of the more dramatic consequences of a low Planck scale, which is possible within theories of extra dimensions, is that black holes could be produced in collider experiments [71] (and by cosmic rays [72]). The black holes would evaporate through Hawking radiation, producing distinct signatures, with a large number of particles in the final state. Note that while the production of black holes require the c.m. energy to be of the order of the (lowered) Planck scale, KK gravitons can be detected at much lower energies.

3.5 Experimental Constraints

Although there exist experimental constraints from collider searches for extra dimensions, these are not strong enough to rule out such theories. Here we will give a short summary of what other kind of constraints on such theories exist.

First there are direct tests of the gravitational inverse-square law (ISL) [13], where one usually puts limits on additional Yukawa contributions, which in the gravitational case have the potential

$$V(r) = -G_N \frac{m_1 m_2}{r} [1 + \alpha e^{-r/\lambda}], \quad (3.29)$$

where α is a dimensionless strength parameter, and λ is a length scale. Such a contribution would be the result of virtual boson exchange, where the mass of the boson, m_b is $1/\lambda$. Such experiments are referred to as table-top experiments and can be performed using a torsion pendulum with an m -fold rotational symmetry placed above an m -fold symmetric rotating attractor. By measuring the torque on the pendulum, regions in the (α, λ) -plane can be excluded. So far, such experiments have been able to exclude the $n = 2$ case of the ADD scenario down to $150 \mu\text{m}$. If the assumption that the extra dimensions should all have the same compactification radius is relaxed, the largest extra dimension still has to be below $200 \mu\text{m}$ [13]. Reaching exclusion limits around $50 \mu\text{m}$ seems to be within reach of this kind of experiments (using current technology).

Then, there are the collider searches, where the most stringent measurements from experiments at the LEP and the Tevatron have resulted in lower bounds on the scale of gravity of the order of 1 TeV for the ADD case as described above. The lower bound on the first graviton excitation in the RS model is of the order of half a TeV [33]. In the years to come, the Tevatron and LHC, and possibly also a linear e^+e^- collider will improve these bounds significantly.

Finally, the most severe constraints to date are the astrophysical and cosmological constraints. If massive KK gravitons exist, they will affect the phenomenology of supernovas and neutron stars. The supernova SN1987A is very interesting in this context. In order for this supernova not to have lost too much energy too quickly, the fundamental gravity scale cannot be lower than $M_D \geq 50 \text{ TeV}$ for $n = 2$, which corresponds to $R < 3 \times 10^{-4} \text{ mm}$. The corresponding numbers for $n = 3$ and $n = 4$ are $M_D \geq 4 \text{ TeV}$ and $M_D \geq 1 \text{ TeV}$, respectively [73]. Furthermore, KK gravitons around neutron stars may decay into SM particles, which could hit the neutron star and lead to excessive heating. Such considerations lead to the even stronger constraints $M_D \geq 1680 \text{ TeV}$ for $n = 2$ and 60 TeV for $n = 3$ [74]. There are uncertainties related to these bounds, but the case of $n = 2$, and probably also the case of $n = 3$ seem to be strongly disfavored if the ADD scenario should help solving the hierarchy problem. For larger n , there are also strong constraints from the absence of neutrino cosmic ray showers produced by black holes [75], where $M_D \geq 1.0\text{--}1.4 \text{ TeV}$ for $n \geq 5$.

Other constraints which will not be presented here come from the cosmic diffuse gamma ray background and early matter domination, but these bounds are weaker than the supernova and neutron star limits mentioned above.

Chapter 4

Comments on the Papers I–IV

In this chapter we shall consider the papers I–IV in more detail. These papers deal with two main topics, namely *graviton-induced bremsstrahlung* (Papers I–III) and the *center–edge asymmetry* (Paper IV). We have studied these topics in the context of both the ADD and the RS models. Common for all four papers is that we take the SM fermions to be massless.

The original ADD and RS scenarios triggered an enormous activity in the field of extra dimensions. As indicated in the previous chapter, the typical discovery channels were the first to be investigated. Several authors considered graviton exchange with two-particle final states. Therefore it seemed both interesting and challenging to consider a three-body final state, such as the bremsstrahlung process, within the framework of extra-dimensional scenarios. Due to an extra coupling of fermions to the photon, such final states will have a significantly lower cross section, but this is the same for both signal and background, so we decided to study the bremsstrahlung process in further detail.

An important issue when it comes to discovering new physics in channels such as the dilepton channel is to be able to distinguish between different models. The center–edge asymmetry is an observable where an asymmetry between events in the ‘center’ and ‘edge’ regions indicates exchange of particles with spin different from 1. This had been investigated in the context of e^+e^- colliders, and it seemed worthwhile to extend this approach to hadron colliders.

Below we give some comments on each of the four papers. Note that in Papers I–III, we use the notation of [19], whereas in Paper IV the notation of [30] is used. In the papers on bremsstrahlung, the notation used was convenient to distinguish between initial- and final-state radiation, whereas in the paper on the center–edge asymmetry, we adopted the Hewett notation since that was the one used in the related e^+e^- collider paper [31].

4.1 Paper I

Paper I, which is published in the *Proceedings of the XVI International Workshop on High Energy Physics and Quantum Field Theory* should be regarded as a first step towards

Paper II. There is therefore some overlap between these two papers, particularly in the introductory parts. In Paper I we discuss the bremsstrahlung process

$$pp \rightarrow \mu^+ \mu^- \gamma + X, \quad (4.1)$$

in the context of the LHC. Here, we only consider the gluon-gluon-fusion contribution to the graviton-exchange process, i.e. the subprocess

$$gg \rightarrow G \rightarrow \mu^+ \mu^- \gamma. \quad (4.2)$$

The reason for choosing the gluon-gluon-fusion channel is the high gluon luminosity at the LHC.

The SM background for the bremsstrahlung process (4.1) comes from quark-antiquark annihilation with the exchange of a photon or a Z . However, in this paper, we neglect the Z exchange, thus we only consider the QED background. Furthermore, we do not consider the initial-state radiation (emission of photons from initial-state quarks). Moreover, we neglect the contribution from quark-antiquark annihilation with graviton exchange, which interferes with the SM background and also has initial state radiation.

The reason for doing these rather crude approximations at this point was to establish a basis for further investigation and to see if the signals one could expect from such graviton exchange processes were detectable, and comparable to the SM background.

To begin with, we focus on the comparison between the bremsstrahlung process (4.1) and the two-body final state process

$$pp \rightarrow \mu^+ \mu^- + X, \quad (4.3)$$

which several authors have considered (see e.g. [30, 33, 58, 65, 66]). To be able to make a correct comparison, we also here neglected the $q\bar{q}$ annihilation with graviton exchange, and calculated the QED background from Feynman diagrams similar to Fig. 3.1 on page 26, with photon exchange instead of graviton exchange. Our result in Eq. (I-4) is in agreement with the result of [68].

The analytic expressions for subprocess cross sections were calculated using the Computer Algebra System REDUCE 3.7 [76]. In Appendix B we include an example of the REDUCE code for obtaining the Feynman amplitude for $gg \rightarrow G \rightarrow \mu^+ \mu^- \gamma$, where we have implemented the Feynman rules for graviton vertices given in [19]. Additional REDUCE programs are needed to find the expressions for the differential cross sections, however, this example should give an impression of the REDUCE syntax. In Appendix B we comment further on our strategy to obtain these expressions.

To fulfill the space limitations of the Proceedings, we found it necessary to remove two of the figures from the original version of Paper I [14] which can be found in the arXiv.org e-Print archive. Since it is the Proceedings version of Paper I which is attached at the end of this thesis, we have included these figures here for the sake of completeness. The notation in the definitions needed to explain these figures will be that of Paper I.

Since we want to investigate the relative magnitude between the graviton contribution and the QED contribution, we first display the ratio between the (parton level) energy

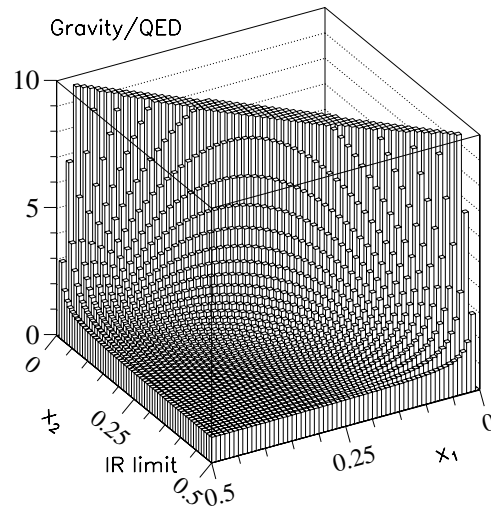


Figure 4.1: Ratio of graviton-induced to QED cross section, *vs.* fractional muon energies x_1 and x_2 . The ratio is normalized to 1 in the IR limit of vanishing photon energy.

distribution of graviton events given in Eq. (I-12) and the QED events given in Eq. (I-27). In Fig. 4.1 we display this ratio in the (x_1, x_2) -plane, where we have normalized to 1 in the IR limit ($x_3 \rightarrow 0$, or $x_1 \simeq x_2 \rightarrow \frac{1}{2}$), where the x_i 's are fractional muon and photon energies. This expression, with the label “Gravity/QED” is

$$\frac{\text{Gravity}}{\text{QED}} = \frac{16x_1x_2 - 6(x_1 + x_2) + 3}{1 - 2x_3}. \quad (4.4)$$

The “wall” at $x_3 \rightarrow \frac{1}{2}$ is due to the collinear singularity that arises from the fourth diagram (see Fig. I-1).

In several of the plots in Paper I, the so-called “figure of merit”, R , is displayed. The dimensionless cross sections, integrated over event shapes subject to y -cuts, which enters in this quantity can be defined as

$$\tilde{\sigma}_{gg \rightarrow \mu^+ \mu^- \gamma}^{(G)} = \iint_{s_i > y\hat{s}} dx_1 dx_2 \frac{Z(x_1, x_2)}{(1 - 2x_1)(1 - 2x_2)(1 - 2x_3)}, \quad (4.5)$$

$$\tilde{\sigma}_{q\bar{q} \rightarrow \mu^+ \mu^- \gamma}^{(\gamma)} = \iint_{s_i > y\hat{s}} dx_1 dx_2 \frac{2(x_1^2 + x_2^2)}{(1 - 2x_1)(1 - 2x_2)}, \quad (4.6)$$

where $Z(x_1, x_2)$ is defined in Eq. (I-9).

In Fig. 4.2 we show the integrated, dimensionless cross sections of Eqs. (4.5) and (4.6) *vs.* x_3^{\min} , where we have integrated over $x_3^{\min} \leq x_3 \leq 0.5$, subject to y -cuts: $s_1, s_2 \geq y\hat{s}$, $s_3 \geq y_3\hat{s}$. Three values of the y -cut are considered, $y = 0.01, 0.02, 0.05$, whereas y_3 , which controls the minimum invariant mass of the two muons, has been held fixed at 0.01.

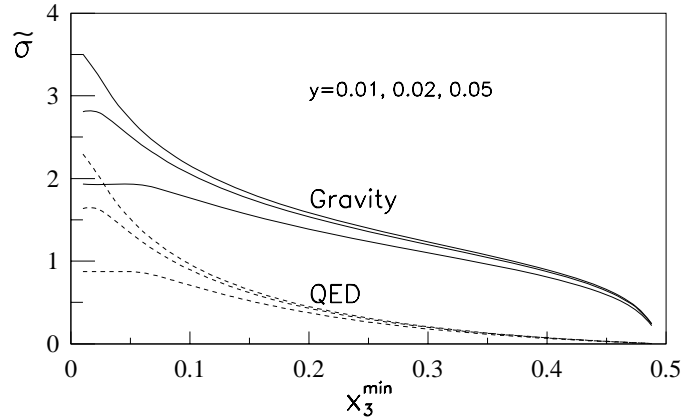


Figure 4.2: Integrated dimensionless cross sections of Eqs. (4.5) and (4.6) vs. x_3^{\min} . Solid: graviton exchange, dashed: QED. Three values of the y -cut are considered, as indicated, from top to bottom.

The numerical results for the over-all process was obtained using the CTEQ5 parton distribution functions [77]. For selected parameters in the ADD and RS models, we calculated the cross section as a function of the (parton) center-of-mass energy, $\sqrt{\hat{s}}$, as well as the figure of merit, R , which is the ratio of the graviton cross section to the QED background.

Note that in the RS case, we integrated over \sqrt{s} in the narrow-width approximation (NWA), which is the reason the sharp peaks do not show up in these plots.

4.2 Paper II

As mentioned above, the topic of this paper is identical to the previous one, where we considered graviton-induced bremsstrahlung at the LHC. After learning that the detectors have higher resolution for electrons than for muons at the LHC, we changed the final state from $\mu^+\mu^-\gamma$ (Paper I) to $e^+e^-\gamma$ (Paper II). This change has no consequence for the results, since we work in the massless fermion limit and take the efficiency to be 1 in both cases.

We extend the calculations in Paper I to include the quark-antiquark annihilation with graviton exchange. Also initial-state radiation (ISR) as well as final-state radiation (FSR) are considered, and for the well known SM background [78] we include both the photon and Z exchange.

When it comes to the analytic expressions for the contributions to the differential (subprocess) cross section, we found it necessary to express the pure ISR contributions [Eqs. (II-3.8) and first line of (II-3.11)] as integrals over $\cos\theta$ [see X_A and X_C in Eqs. (II-A4) and (II-A5)], where θ is the scattering angle in the c.m. frame. The reason is that

they, in contrast to the other contributions, are not polynomials in $\cos\theta$ because of the initial-state fermion propagator.

Based on the analytic parton cross sections, differential with respect to x_1 and x_2 , together with the (CTEQ5) parton distribution functions, we perform numerical integrations to obtain results for the over-all cross section, differential in $\sqrt{\hat{s}}$. We also study the photon perpendicular momentum spectrum, where we integrate out the $\sqrt{\hat{s}}$ dependence. Note that this spectrum has no analogue in the two-body process.

In the RS scenario, where the graviton resonances result in sharp peaks in the cross section, we also performed a bin-integration which indicated that it should be possible to resolve such resonances at the LHC.

4.3 Paper III

The topic of Paper III is graviton-induced bremsstrahlung at e^+e^- colliders, thus its context is different from the other papers which focus on hadron colliders. Although the collision energy is lower at an e^+e^- collider compared to that of hadron colliders, there are several advantages. First of all the environment is cleaner, thus much higher precision can be reached. Furthermore, the ability to tune the collision energy is also valuable, together with the possibility of having polarized beams. The collision energy is also (to a good approximation) the same for all events in contrast to the parton collisions at hadron colliders.

The notation used here is the same as in Paper II, except for a few modifications such as $X_A \rightarrow X_{AA}$ etc. This paper contains complete analytic expressions for the angular distributions of the bremsstrahlung process

$$e^+e^- \rightarrow \mu^+\mu^-\gamma, \quad (4.7)$$

given by the differential cross sections with respect to x_3 , $\eta = x_1 - x_2$ and $\cos\theta$. The reason we return to the $\mu^+\mu^-\gamma$ final state is to avoid the more involved Bhabha scattering process, which also has t -channel in addition to s -channel exchange.

Except charge normalization factors, the cross section expressions for the process in Eq. (4.7) are similar to those of the subprocess $q\bar{q} \rightarrow e^+e^-\gamma$ at hadron colliders [15]. The gluon-gluon fusion process on the other hand has no analogue at e^+e^- colliders, but a photon-photon collider would have analogous channels.

In both the ADD and RS scenarios, we consider total cross sections, photon perpendicular momentum and angular distributions at various collider energies, such as $\sqrt{s} = 0.5, 1, 3$ and 5 TeV. The photon perpendicular momentum distribution is particularly interesting in the RS case, where the possibility of radiative return to lower-lying graviton resonances is demonstrated.

Previously, the process $e^+e^- \rightarrow \gamma\nu\bar{\nu}$, which also is a three-body process has been investigated by Kumar Rai et al. [79]. Since the neutrinos are not detected, the signature of this process is a single hard transverse photon with missing energy. By comparing this final-state to the $\mu^+\mu^-$ final-state a distinction between the ADD and RS case is possible,

even in the regions of parameter space which give very broad RS resonances. The idea is that in the ADD model, both the $\mu^+\mu^-$ and $\gamma + \cancel{E}_T$ are $2 \rightarrow 2$ body processes, whereas in the RS model, the $\gamma + \cancel{E}_T$ is a $2 \rightarrow 3$ body process, which is phase-space suppressed. Comparing the Feynman diagrams of the γe^+e^- and $\gamma\nu\bar{\nu}$ processes, we see that there is a background process with W exchange in the latter. Furthermore, the FSR diagrams are not present.

A short review of Paper III, based on a talk given at the *International Workshop on Physics and Experiments with Future Electron-Positron Linear Colliders* (LCWS 2004), held in Paris will appear in the Proceedings of this conference [80].

4.4 Paper IV

The contents of Paper IV are rather different from the other papers, since we here are concerned with an asymmetry related to two-body final-states (both e^+e^- and $\mu^+\mu^-$), the so-called center–edge asymmetry. This observable has previously been investigated in the context of e^+e^- colliders [31], and here we adapt this approach to hadron colliders. The most intuitive definition of this asymmetry is the following

$$A_{\text{CE}} = \frac{N_{\text{center}} - N_{\text{edge}}}{N_{\text{center}} + N_{\text{edge}}}, \quad (4.8)$$

where N_{center} and N_{edge} are the numbers of events in the center and edge regions respectively. Events can be categorized according to the cosine of their scattering angle (in the c.m. frame) as

$$\begin{aligned} \text{Center region:} & \quad |z| = |\cos\theta| \leq z^*, \\ \text{Edge region:} & \quad |z| = |\cos\theta| > z^*, \end{aligned} \quad (4.9)$$

where z^* is an arbitrary parameter between 0 and 1. In Fig. 4.3 an illustration of the center and edge regions for a specific choice of z^* is given.

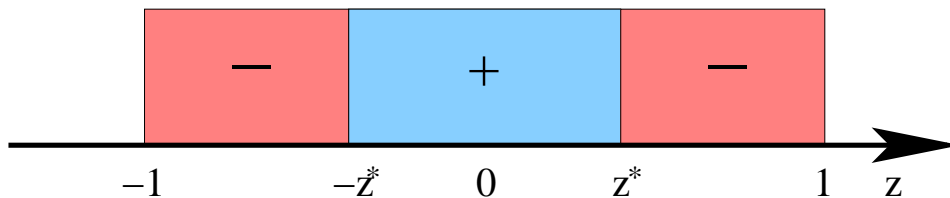


Figure 4.3: Center (+) and edge (−) regions defined by z^* , where $z = \cos\theta$ and θ is the c.m. scattering angle.

When no cuts are imposed, $A_{\text{CE}}^{\text{spin-1}}$ vanishes for $z^* = z_0^* \simeq 0.596$. However, when cuts are imposed, things become more complicated. In Paper IV we focus on how to define z^* such

that the center–edge asymmetry vanishes for spin-1 exchange. Two methods are discussed, one rapidity-dependent approach, based on the analytic solution of a cubic equation, and another numerical approach which depends on the invariant mass, M , of the lepton pair in the final state. Since the M -dependent approach is sensitive to the bin-width, the rapidity-dependent approach is found to give the most precise cancellation of the spin-1 component of the center-edge asymmetry.

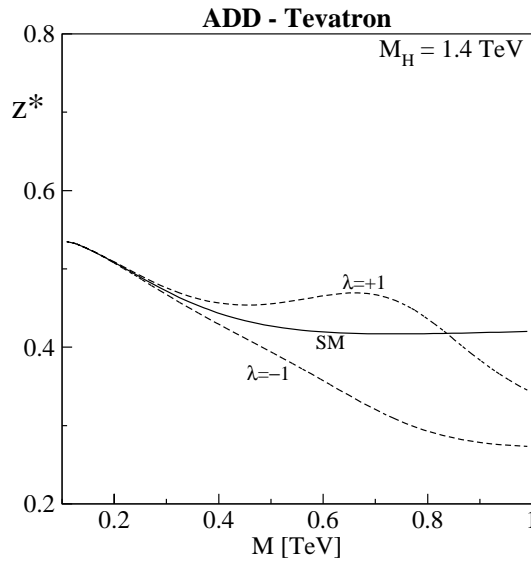


Figure 4.4: Zeros of A_{CE} and their M dependence at the Tevatron. The solid curves give z_0^* , which corresponds to $A_{CE}^{SM} = 0$, whereas the dashed curves correspond to $A_{CE} = 0$ for the ADD model, with $M_H = 1.4$ TeV and $\lambda = \pm 1$ at the Tevatron.

For completeness, we shall here include the Tevatron version of Fig. IV-7, where we display the zeros of A_{CE} and their M -dependence, with M being the invariant mass of the lepton pair. In Fig. 4.4, we display z_0^* at the Tevatron where the cuts are more complicated than at the LHC. This leads to a different behavior, with decreasing z_0^* as M increases (compare Fig. IV-7). We do not intend to give an explanation of this behavior here, although it can be understood from the same considerations as in the LHC case.

The value of z^* , for which the center–edge asymmetry vanishes, is related to the angular distribution, which is determined by the spin of the exchanged particle. Therefore, if we can remove the SM contribution by a proper choice of z^* , we have succeeded in removing all spin-1-based new-physics contributions to the center–edge asymmetry. Observing a non-zero A_{CE} would therefore indicate exchange of particles with spin different from 1. Since the spin of a graviton is 2, the center–edge asymmetry may turn out to be useful when searching for signs of extra dimensions. As pointed out in Paper IV, this approach is an alternative to a fit to the angular distribution, which seems worthwhile exploring, in particular if the statistics are limited.

In Paper IV, we use the center-edge asymmetry to obtain spin-2 identification limits in both the ADD and RS scenarios, using the CTEQ6 parton distribution functions [81].

Chapter 5

Summary and Conclusion

In this thesis we have considered different aspects of theories of extra space dimensions, with special emphasis on the ADD and RS models. Four research papers have been presented, treating the two topics

- Graviton-induced bremsstrahlung at both hadron and e^+e^- colliders
- Center-edge asymmetry at hadron colliders

The introductory chapters were aimed at deriving Feynman rules for massive gravitons, which are present in theories of extra dimensions. Moreover, we presented some features of the ADD and RS scenarios, and mentioned briefly some alternative scenarios based on the existence of extra dimensions. The phenomenological aspects of such theories, together with the experimental constraints have also been reviewed, and finally a few comments on the four research papers attached at the end of this thesis were made.

In the case of graviton-induced bremsstrahlung (Papers I–III), analytic expressions for differential cross sections have been presented for both initial- and final-state radiation. We focused in particular on the photon perpendicular momentum spectrum, which is characteristic for the three-body process and has no analogue in the two-body final state. Although the bremsstrahlung process is suppressed compared to processes with only two particles in the final state, and therefore is unlikely to be one of the discovery channels, it may still be worthwhile searching for such events since they can provide additional confirmation on the underlying physics.

The paper on center-edge asymmetry at hadron colliders (Paper IV) extended previous work by Osland, Pankov and Paver who considered this observable in the context of two-body final states at e^+e^- colliders. At hadron colliders it turned out that obtaining a vanishing SM contribution to the center-edge asymmetry is not straightforward. We considered two different approaches, one rapidity-dependent and one which depends on the invariant mass of the lepton pair, and concluded that the rapidity-dependent approach was the most reliable one, since it is based on an explicit analytic expression.

Questions related to the existence of extra dimensions are indeed very profound for our understanding of the universe, and in the years to come, the search for extra space dimensions will continue with increasing pace. When the LHC is turned on, many of the theories

mentioned in this thesis will be challenged and ruled out by experimental observations. However, if indications of the existence of extra dimensions are finally found, the universe in which we live will turn out to be remarkably different from what it apparently looks like.

Appendix A

Feynman Rules

Here we present a summary of the Feynman rules for the graviton propagator, and for the massive graviton vertices which was derived in Chapt. 2. For simplicity, we define [19]

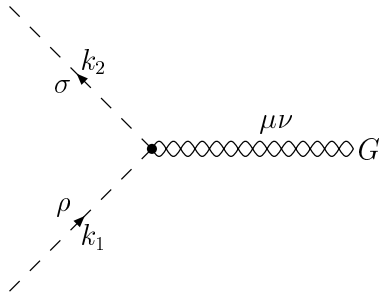
$$\begin{aligned}
 C_{\mu\nu\rho\sigma} &= \eta_{\mu\rho}\eta_{\nu\sigma} + \eta_{\mu\sigma}\eta_{\nu\rho} - \eta_{\mu\nu}\eta_{\rho\sigma}, \\
 D_{\mu\nu\rho\sigma}(k_1, k_2) &= \eta_{\mu\nu}k_{1\sigma}k_{2\rho} \\
 &\quad - (\eta_{\mu\sigma}k_{1\nu}k_{2\rho} + \eta_{\mu\rho}k_{1\sigma}k_{2\nu} - \eta_{\rho\sigma}k_{1\mu}k_{2\nu}) \\
 &\quad - (\eta_{\nu\sigma}k_{1\mu}k_{2\rho} + \eta_{\nu\rho}k_{1\sigma}k_{2\mu} - \eta_{\rho\sigma}k_{1\nu}k_{2\mu}),
 \end{aligned} \tag{A.1}$$

in order to have a more compact notation in the vertex rules given below.



$$\frac{i(\eta_{\mu\rho}\eta_{\nu\sigma} + \eta_{\mu\sigma}\eta_{\nu\rho} - \frac{2}{3}\eta_{\mu\nu}\eta_{\rho\sigma})}{k^2 - m_{\bar{g}}^2 + i\varepsilon}$$

Figure A.1: Feynman rule for the graviton propagator.



$$-i\frac{\kappa}{2}(m_{\Phi}^2\eta_{\mu\nu} + C_{\mu\nu\rho\sigma}k_1^\rho k_2^\sigma)$$

Figure A.2: Feynman rule for the scalar-scalar-graviton vertex.

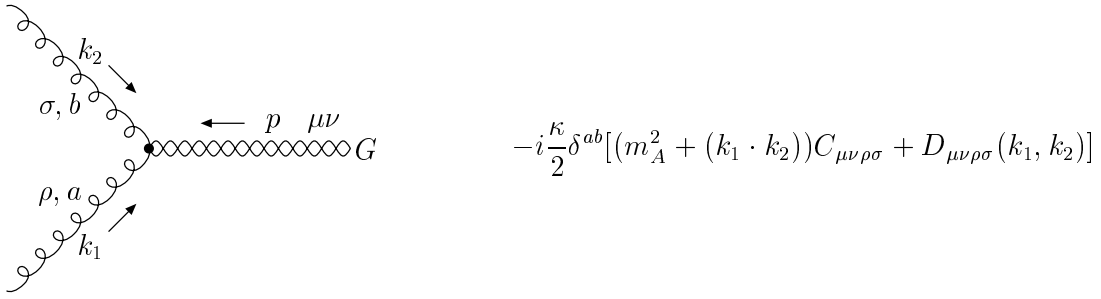


Figure A.3: Feynman rule for the vector-vector-graviton vertex. The abelian case does not require a Kronecker-delta.

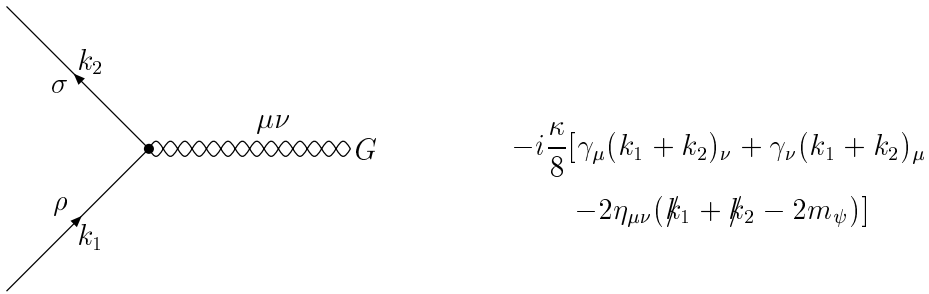


Figure A.4: Feynman rule for the fermion-fermion-graviton vertex.

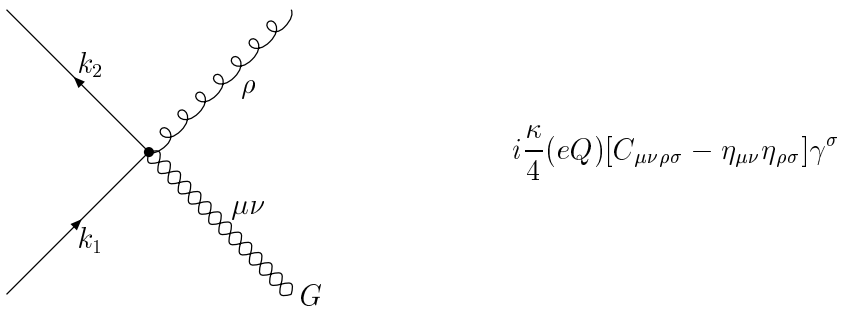


Figure A.5: Feynman rule for the fermion-fermion-vector-graviton vertex.

Appendix B

REDUCE Program Example

In this appendix, we display parts of the REDUCE [76] program `gg-grav.red` used to calculate the Feynman amplitude and finally also the analytical expressions for the cross section of the bremsstrahlung process $gg \rightarrow G \rightarrow \mu^+ \mu^- \gamma$. This is where the Feynman rules are implemented, and the Feynman amplitudes are constructed.

After running this program, the strategy was to manipulate the ordering of gamma matrices such that the hermitian conjugate of the amplitude could be obtained easily. A separate program then reads in the amplitude and its hermitian conjugate, multiplies them together and takes the trace. An analytic expression for the differential cross section is then obtained, and integration over the variables which are easy to integrate out is performed. We are left with expressions which are presented in both Papers I and II.

The case of fermions is more complicated, since there are two fermion-lines involved. It is important to keep these apart in REDUCE by using the `nospur` command until traces are taken, since otherwise REDUCE would take the trace of the whole expression instead of multiplying two traces.

```
#####Started April 2001#####
% Consider gluon-gluon fusion diagrams
#####
% To start reduce:
% reduce
% To run this program:
% 1: in "filename";
% To leave REDUCE:
% 2: bye;
#####

off nat$

vecdim 4$
```

```

array ampl(4)$

% Declare operators:
operator cc,dd,ee$
operator graviton_gg,graviton_ff_a,graviton_ff,pr_graviton,
      graviton_gaga,pr_gamma$
operator fermion_photon,prq$

% Declare vectors:
vector k1,k2,p1,p2,k$
vector p,q$
vector k01,k02,mu0,nu0,rho0,sigma0,sigma00$
vector mu,nu,rho,sigma,mu1,nu1,mu2,nu2,rho1,sigma0,sigma1,rho2$
vector mu1pr,mu2pr,nupr,lambda,lambdapr$
vector tau1,tau2,omega1,omega2$
vector alpha,beta,gamma,alpha1,beta1,gamma1$

nospur ll$
%=====

% Define C, D, E (according to Han et al.):

for all mu0,nu0,rho0,sigma0
let cc(mu0,nu0,rho0,sigma0)
=mu0.rho0*nu0.sigma0+mu0.sigma0*nu0.rho0-mu0.nu0*rho0.sigma0$

for all mu0,nu0,rho0,sigma0,k01,k02
let dd(mu0,nu0,rho0,sigma0,k01,k02)
=mu0.nu0*k01.sigma0*k02.rho0
-(mu0.sigma0*k01.nu0*k02.rho0+mu0.rho0*k01.sigma0*k02.nu0
-rho0.sigma0*k01.mu0*k02.nu0
+nu0.sigma0*k01.mu0*k02.rho0+nu0.rho0*k01.sigma0*k02.mu0
-rho0.sigma0*k01.nu0*k02.mu0)$

for all mu0,nu0,rho0,sigma0,k01,k02
let ee(mu0,nu0,rho0,sigma0,k01,k02)
=mu0.nu0*(k01.rho0*k01.sigma0+k02.rho0*k02.sigma0+k01.rho0*k02.sigma0)
-(nu0.sigma0*k01.mu0*k01.rho0+nu0.rho0*k02.mu0*k02.sigma0
+mu0.sigma0*k01.nu0*k01.rho0+mu0.rho0*k02.nu0*k02.sigma0)$

%=====
% FEYNMAN RULES (according to Han et al.)

%Graviton-gluon-gluon vertex (Figure 4):
% gluons: (k01,rho0), (k02,sigma0)

```

```

% graviton: (mu0,nu0)

for all k01,k02,rho0,sigma0,mu0,nu0
let graviton_gg(k01,k02,rho0,sigma0,mu0,nu0)
=-i*(kappa/2)*(k01.k02*cc(mu0,nu0,rho0,sigma0)
      +dd(mu0,nu0,rho0,sigma0,k01,k02)
      +xi_inv*ee(mu0,nu0,rho0,sigma0,k01,k02))$

%Graviton-photon-photon vertex (Figure 4):
% photons: (k01,rho0), (k02,sigma0)
% graviton: (mu0,nu0)

for all k01,k02,rho0,sigma0,mu0,nu0
let graviton_gaga(k01,k02,rho0,sigma0,mu0,nu0)
=-i*(kappa/2)*(k01.k02*cc(mu0,nu0,rho0,sigma0)
      +dd(mu0,nu0,rho0,sigma0,k01,k02)
      +xi_inv*ee(mu0,nu0,rho0,sigma0,k01,k02))$

%Graviton-fermion-fermion vertex (Figure 4):
% graviton: (mu0,nu0)
% fermions: (k01 in, k02 out)

for all l1,mu0,nu0,k01,k02
let graviton_ff(l1,mu0,nu0,k01,k02)
=-i*(kappa/8)*(G(l1,mu0)*(k01.nu0+k02.nu0)+G(l1,nu0)*(k01.mu0+k02.mu0)
      -2*mu0.nu0*(G(l1,k01)+G(l1,k02)-2*mf))$

%Graviton-fermion-fermion-photon vertex (Figure 5):
% graviton: (mu0,nu0)
% photon: (rho0)

for all l1,mu0,nu0,rho0
let graviton_ff_a(l1,mu0,nu0,rho0)
=+i*qf*(kappa/4)*(cc(mu0,nu0,rho0,sigma00)-mu0.nu0*rho0.sigma00)
      *G(l1,sigma00)$

%Graviton propagator (leave out denominator):

for all mu0,nu0,rho0,sigma0
let pr_graviton(mu0,nu0,rho0,sigma0)
=i*(mu0.rho0*nu0.sigma0+mu0.sigma0*nu0.rho0-(2/3)*mu0.nu0*rho0.sigma0)$

% Fermion-photon vertex:

for all l1,mu0

```

```

let fermion_photon(l1,mu0)=-i*qf*G(l1,mu0)$

% Fermion propagator:

for all l1,k01
let prq(l1,k01)=i*(G(l1,k01) + mf)/(k01.k01-mf**2)$

% Photon propagator:

for all mu0,nu0,k01
let pr_gamma(mu0,nu0,k01)=-i*mu0.nu0/(k01.k01)$

%=====

% Now construct amplitudes for four diagrams:

% Couplings with graviton-fermion-fermion vertex:

amplitude1:=graviton_gg(k1,k2,mu1,mu2,tau1,tau2)
            *pr_graviton(tau1,tau2,omega1,omega2)
            *fermion_photon(l1,nu)
            *prq(l1,p1+k)
            *graviton_ff(l1,omega1,omega2,-p2,p1+k)$

amplitude2:=graviton_gg(k1,k2,mu1,mu2,tau1,tau2)
            *pr_graviton(tau1,tau2,omega1,omega2)
            *graviton_ff(l1,omega1,omega2,-p2-k,p1)
            *prq(l1,-p2-k)
            *fermion_photon(l1,nu)$

% Coupling with graviton-fermion-fermion-photon vertex:

amplitude3:=graviton_gg(k1,k2,mu1,mu2,tau1,tau2)
            *pr_graviton(tau1,tau2,omega1,omega2)
            *graviton_ff_a(l1,omega1,omega2,nu)$

% Coupling with graviton-photon-photon vertex:

amplitude4:=graviton_gg(k1,k2,mu1,mu2,tau1,tau2)
            *pr_graviton(tau1,tau2,omega1,omega2)
            *graviton_gaga(k,p1+p2,nu,lambda,omega1,omega2)
            *pr_gamma(lambda,lambdapr,p1+p2)
            *fermion_photon(l1,lambdapr)$

% All four amplitudes:

```



```

ampl(1):=amplitude1$
ampl(2):=amplitude2$
ampl(3):=amplitude3$
ampl(4):=amplitude4$

%=====

% Suppress the factor  $i\kappa^2 qf$  which appears in all amplitudes:

for j1:=1 step 1 until 4 do
begin
ampl(j1):=ampl(j1)/(i*kappa**2*qf)$
end$

% When a vector is declared as an index, REDUCE will automatically
% perform a summation over that index

index sigma00$
for j1:=1 step 1 until 4 do
begin
ampl(j1):=ampl(j1)$
end$

pause$

index tau1,tau2,omega1,omega2$
for j1:=1 step 1 until 4 do
begin
ampl(j1):=ampl(j1)$
end$

index lambda,lambdapr$
let k.k=0, xi_inv=0$
for j1:=1 step 1 until 4 do
begin
ampl(j1):=ampl(j1)$
end$

factor G$

for j1:=1 step 1 until 4 do
begin
ampl(j1):=ampl(j1)$
end$

```

```
pause$

% Apply Dirac equation:
let G(l1,p1)= mf,
    G(l1,p2)=-mf$

for j1:=1 step 1 until 4 do
begin
ampl(j1):=ampl(j1)$
end$

% Sum all amplitudes:

amplitude:=ampl(1)+ampl(2)+ampl(3)+ampl(4);

% Write to file:

out "gg-mumuga-out.res";
amplitude:=amplitude;
;end$

shut "gg-mumuga-out.res";

% Stop here!
end$
```

Bibliography

- [1] I. Newton, *Philosophiæ naturalis principia mathematica* (William Dawson, London, 1687).
- [2] G. Nordstrom, Phys. Z. **13**, 1126 (1912).
- [3] G. Nordstrom, Phys. Z. **15**, 504 (1914).
- [4] A. Einstein, Annalen Phys. **49**, 769 (1916).
- [5] T. Kaluza, Sitzungsber. Preuss. Akad. Wiss. Berlin (Math. Phys.) **1921**, 966 (1921).
- [6] O. Klein, Z. Phys. **37**, 895 (1926) [Surveys High Energ. Phys. **5**, 241 (1986)].
- [7] K. Akama, Lect. Notes Phys. **176**, 267 (1982) [arXiv:hep-th/0001113].
- [8] V. A. Rubakov and M. E. Shaposhnikov, Phys. Lett. B **125**, 136 (1983); Phys. Lett. B **125**, 139 (1983).
- [9] M. Visser, Phys. Lett. B **159**, 22 (1985) [arXiv:hep-th/9910093].
- [10] I. Antoniadis, Phys. Lett. B **246**, 377 (1990).
- [11] I. Antoniadis, K. Benakli and M. Quiros, Phys. Lett. B **331**, 313 (1994) [arXiv:hep-ph/9403290].
- [12] N. Arkani-Hamed, S. Dimopoulos and G. R. Dvali, Phys. Lett. B **429**, 263 (1998) [arXiv:hep-ph/9803315].
- [13] C. D. Hoyle, U. Schmidt, B. R. Heckel, E. G. Adelberger, J. H. Gundlach, D. J. Kapner and H. E. Swanson, Phys. Rev. Lett. **86**, 1418 (2001) [arXiv:hep-ph/0011014];
E. G. Adelberger [EOT-WASH Group Collaboration], arXiv:hep-ex/0202008;
E. G. Adelberger, B. R. Heckel and A. E. Nelson, Ann. Rev. Nucl. Part. Sci. **53**, 77 (2003) [arXiv:hep-ph/0307284]; E. G. Adelberger, J. H. Gundlach, U. Schmidt and H. E. Swanson, arXiv:hep-ph/0405262.
- [14] E. Dvergsnes, P. Osland and N. Öztürk, in *Proceedings of 16th International Workshop on High Energy Physics and Quantum Field Theory (QFTHEP 2001)*, edited by M.N. Dubinin and V.I. Savrin, Moscow, Russia, Skobeltsyn Inst. Nucl. Phys., 2001, pp. 54-63, arXiv:hep-ph/0108029.
- [15] E. Dvergsnes, P. Osland and N. Öztürk, Phys. Rev. D **67**, 074003 (2003) [arXiv:hep-ph/0207221];

- [16] T. Buanes, E. W. Dvergsnes and P. Osland, *Eur. Phys. J. C* **35**, 555 (2004) [arXiv:hep-ph/0403267].
- [17] E. W. Dvergsnes, P. Osland, A. A. Pankov and N. Paver, *Phys. Rev. D* **69**, 115001 (2004) [arXiv:hep-ph/0401199].
- [18] G. F. Giudice, R. Rattazzi and J. D. Wells, *Nucl. Phys. B* **544**, 3 (1999) [arXiv:hep-ph/9811291].
- [19] T. Han, J. D. Lykken and R. J. Zhang, *Phys. Rev. D* **59**, 105006 (1999) [arXiv:hep-ph/9811350].
- [20] C. Csaki, arXiv:hep-ph/0404096.
- [21] H. van Dam and M. J. G. Veltman, *Nucl. Phys. B* **22**, 397 (1970); V. I. Zakharov, *Sov. Phys. JETP Lett.* **12** 312 (1970).
- [22] F. Mandl and G. Shaw, *Quantum Field Theory* (John Wiley & Sons, New York, 1996).
- [23] Y. A. Kubyshin, arXiv:hep-ph/0111027.
- [24] V. A. Rubakov, *Phys. Usp.* **44**, 871 (2001) [*Usp. Fiz. Nauk* **171**, 913 (2001)] [arXiv:hep-ph/0104152].
- [25] J. Hewett and M. Spiropulu, *Ann. Rev. Nucl. Part. Sci.* **52**, 397 (2002) [arXiv:hep-ph/0205106].
- [26] A. V. Kisselev, arXiv:hep-ph/0303090.
- [27] K. Cheung, arXiv:hep-ph/0305003.
- [28] J. K. Hoskins, R. D. Newman, R. Spero and J. Schultz, *Phys. Rev. D* **32**, 3084 (1985).
- [29] N. Arkani-Hamed, S. Dimopoulos and G. R. Dvali, *Phys. Rev. D* **59**, 086004 (1999) [arXiv:hep-ph/9807344].
- [30] J. L. Hewett, *Phys. Rev. Lett.* **82**, 4765 (1999) [arXiv:hep-ph/9811356].
- [31] P. Osland, A. A. Pankov and N. Paver, *Phys. Rev. D* **68**, 015007 (2003) [arXiv:hep-ph/0304123].
- [32] L. Randall and R. Sundrum, *Phys. Rev. Lett.* **83**, 3370 (1999) [arXiv:hep-ph/9905221].
- [33] H. Davoudiasl, J. L. Hewett and T. G. Rizzo, *Phys. Rev. Lett.* **84**, 2080 (2000) [arXiv:hep-ph/9909255].
H. Davoudiasl, J. L. Hewett and T. G. Rizzo, *Phys. Rev. D* **63**, 075004 (2001) [arXiv:hep-ph/0006041].
- [34] *Handbook of Mathematical Functions with Formulas, Graphs, and Mathematical tables*, ed. by M. Abramowitz and I. A. Stegun, Dover Publications, Inc., New York (9th printing, 1970).

- [35] M. Chaichian, A. Datta, K. Huitu and Z. h. Yu, Phys. Lett. B **524**, 161 (2002) [arXiv:hep-ph/0110035].
- [36] K. R. Dienes, E. Dudas and T. Gherghetta, Phys. Lett. B **436**, 55 (1998) [arXiv:hep-ph/9803466].
- [37] L. Randall and R. Sundrum, Phys. Rev. Lett. **83**, 4690 (1999) [arXiv:hep-th/9906064].
- [38] S. Chang, J. Hisano, H. Nakano, N. Okada and M. Yamaguchi, Phys. Rev. D **62**, 084025 (2000) [arXiv:hep-ph/9912498].
- [39] H. Collins and B. Holdom, Phys. Rev. D **64**, 064003 (2001) [arXiv:hep-ph/0103103].
- [40] I. I. Kogan, S. Mouslopoulos, A. Papazoglou, G. G. Ross and J. Santiago, Nucl. Phys. B **584**, 313 (2000) [arXiv:hep-ph/9912552].
- [41] N. Arkani-Hamed, S. Dimopoulos, G. R. Dvali and N. Kaloper, Phys. Rev. Lett. **84**, 586 (2000) [arXiv:hep-th/9907209].
- [42] P. Binetruy, C. Deffayet and D. Langlois, Nucl. Phys. B **565**, 269 (2000) [arXiv:hep-th/9905012]; D. Ida, JHEP **0009**, 014 (2000) [arXiv:gr-qc/9912002].
- [43] J. Khoury, B. A. Ovrut, P. J. Steinhardt and N. Turok, Phys. Rev. D **64**, 123522 (2001) [arXiv:hep-th/0103239].
- [44] T. Appelquist, H. C. Cheng and B. A. Dobrescu, Phys. Rev. D **64**, 035002 (2001) [arXiv:hep-ph/0012100].
- [45] N. Arkani-Hamed, S. Dimopoulos, G. R. Dvali and J. March-Russell, Phys. Rev. D **65**, 024032 (2002) [arXiv:hep-ph/9811448]; G. R. Dvali and A. Y. Smirnov, Nucl. Phys. B **563**, 63 (1999) [arXiv:hep-ph/9904211].
- [46] S. M. Carroll and M. M. Guica, arXiv:hep-th/0302067.
- [47] N. Arkani-Hamed, A. G. Cohen and H. Georgi, Phys. Rev. Lett. **86**, 4757 (2001) [arXiv:hep-th/0104005].
- [48] E. A. Mirabelli, M. Perelstein and M. E. Peskin, Phys. Rev. Lett. **82**, 2236 (1999) [arXiv:hep-ph/9811337].
- [49] V. M. Abazov *et al.* [D0 Collaboration], Phys. Rev. Lett. **90**, 251802 (2003) [arXiv:hep-ex/0302014].
- [50] D. Acosta *et al.* [CDF Collaboration], Phys. Rev. Lett. **89**, 281801 (2002) [arXiv:hep-ex/0205057].
- [51] J. Abdallah [DELPHI Collaboration], arXiv:hep-ex/0406019.
- [52] T. Han, D. L. Rainwater and D. Zeppenfeld, Phys. Lett. B **463**, 93 (1999) [arXiv:hep-ph/9905423].
- [53] D. Atwood, S. Bar-Shalom and A. Soni, arXiv:hep-ph/9903538.

- [54] O. J. P. Eboli, M. B. Magro, P. Mathews and P. G. Mercadante, Phys. Rev. D **64**, 035005 (2001) [arXiv:hep-ph/0103053].
- [55] O. J. P. Eboli, T. Han, M. B. Magro and P. G. Mercadante, Phys. Rev. D **61**, 094007 (2000) [arXiv:hep-ph/9908358].
- [56] K. m. Cheung, Phys. Rev. D **61**, 015005 (2000) [arXiv:hep-ph/9904266].
- [57] LEPWWG $f\bar{f}$ SubGroup (C. Geweniger *et. al.*), Combination of the LEP II $f\bar{f}$ Results, CERN preprint LEP2FF/02-03 (October 2002).
- [58] K. m. Cheung and G. Landsberg, Phys. Rev. D **62**, 076003 (2000) [arXiv:hep-ph/9909218].
- [59] B. Abbott *et al.* [D0 Collaboration], Phys. Rev. Lett. **86**, 1156 (2001) [arXiv:hep-ex/0008065].
- [60] M. A. Doncheski, in *Proc. of the APS/DPF/DPB Summer Study on the Future of Particle Physics (Snowmass 2001)* ed. N. Graf, eConf **C010630**, P314 (2001) [arXiv:hep-ph/0111149].
- [61] T. G. Rizzo, Phys. Rev. D **60**, 075001 (1999) [arXiv:hep-ph/9903475].
- [62] K. Agashe and N. G. Deshpande, Phys. Lett. B **456**, 60 (1999) [arXiv:hep-ph/9902263].
- [63] P. Mathews, S. Raychaudhuri and K. Sridhar, Phys. Lett. B **450**, 343 (1999) [arXiv:hep-ph/9811501].
- [64] S. Chang and M. Yamaguchi, arXiv:hep-ph/9909523.
- [65] P. Traczyk and G. Wrochna, arXiv:hep-ex/0207061;
C. Collard, M.-C. Lemaire, P. Traczyk, G. Wrochna, CMS NOTE-2002/050
- [66] B. C. Allanach, K. Odagiri, M. A. Parker and B. R. Webber, JHEP **0009**, 019 (2000) [arXiv:hep-ph/0006114]; B. C. Allanach, K. Odagiri, M. J. Palmer, M. A. Parker, A. Sabetfakhri and B. R. Webber, JHEP **0212**, 039 (2002) [arXiv:hep-ph/0211205].
- [67] T. G. Rizzo, JHEP **0210**, 013 (2002) [arXiv:hep-ph/0208027].
- [68] J. Bijnens, P. Eerola, M. Maul, A. Mansson and T. Sjostrand, Phys. Lett. B **503**, 341 (2001) [arXiv:hep-ph/0101316].
- [69] G. Azuelos, P. H. Beauchemin and C. P. Burgess, arXiv:hep-ph/0401125.
- [70] G. F. Giudice, R. Rattazzi and J. D. Wells, Nucl. Phys. B **595**, 250 (2001) [arXiv:hep-ph/0002178].
- [71] S. B. Giddings and S. Thomas, Phys. Rev. D **65**, 056010 (2002) [arXiv:hep-ph/0106219];
S. Dimopoulos and G. Landsberg, Phys. Rev. Lett. **87**, 161602 (2001) [arXiv:hep-ph/0106295].
- [72] J. L. Feng and A. D. Shapere, Phys. Rev. Lett. **88**, 021303 (2002) [arXiv:hep-ph/0109106].
- [73] S. Cullen and M. Perelstein, Phys. Rev. Lett. **83**, 268 (1999) [arXiv:hep-ph/9903422].

- [74] S. Hannestad and G. G. Raffelt, *Phys. Rev. Lett.* **88**, 071301 (2002) [arXiv:hep-ph/0110067].
- [75] L. A. Anchordoqui, J. L. Feng, H. Goldberg and A. D. Shapere, *Phys. Rev. D* **68**, 104025 (2003) [arXiv:hep-ph/0307228].
- [76] Anthony C. Hearn, *REDUCE User's Manual 3.6*, RAND Publication CP78 (1995).
On-line manual:
<http://www.uni-koeln.de/REDUCE/3.6/doc/reduce>
<http://www.zib.de/Symbolik/reduce/moredocs/reduce.pdf>
- [77] H. L. Lai *et al.* [CTEQ Collaboration], *Eur. Phys. J. C* **12**, 375 (2000) [arXiv:hep-ph/9903282].
- [78] F. A. Berends and R. Kleiss, *Nucl. Phys. B* **177**, 237 (1981); F. A. Berends, R. Kleiss and S. Jadach, *Nucl. Phys. B* **202**, 63 (1982).
- [79] S. Kumar Rai and S. Raychaudhuri, *JHEP* **0310**, 020 (2003) [arXiv:hep-ph/0307096].
- [80] T. Buanes, E. W. Dvergsnes and P. Osland, arXiv:hep-ph/0408063.
- [81] J. Pumplin, D. R. Stump, J. Huston, H. L. Lai, P. Nadolsky and W. K. Tung, *JHEP* **0207**, 012 (2002) [arXiv:hep-ph/0201195].